State University of New York Report

LES, DNS and RANS for the Analysis of High-Speed Turbulent Reacting Flows

by

P.J. Colucci, F.A. Jaberi
and P. Givi

Department of Mechanical and Aerospace Engineering
State University of New York at Buffalo
Buffalo, New York 14260-4400

Annual Report Submitted to
NASA Langley Research Center

Progress Report on Activities Supported Under Grant NAG 1-1122

for the Period

August 1, 1995 - July 31, 1996

Contents

LES, DNS and RANS for the Analysis of High-Speed Turbulent Reacting Flows

P.J. Colucci, F.A. Jaberi and P. Givi
Department of Mechanical and Aerospace Engineering
State University of New York
Buffalo, NY 14260-4400

Abstract

The purpose of this research is to continue our efforts in advancing the state of knowledge in large eddy simulation (LES), direct numerical simulation (DNS) and Reynolds averaged Navier Stokes (RANS) methods for the computational analysis of high-speed reacting turbulent flows. We have just finished the third year of Phase II of this research. This report provides a detailed description of our most recent findings in the research supported under this program.

Technical Monitor:

Dr. J. Philip Drummond (Hypersonic Propulsion Branch, NASA LaRC, Mail Stop 197, Tel: 804-864-2298) is the Technical Monitor of this Grant.

1 Introduction

We have just finished Year 3 of Phase II activities on this NASA LaRC sponsored project. The total time allotted for this phase is three years; this phase was followed at the conclusion of Phase I activities (also for three years). Thus, in total we have completed 6 years of LaRC supported research. A proposal for continuation of these efforts is pending at the NASA LaRC.

Our work in this project can be divided into the following categories: (1) development of LES methodologies via PDF methods and numerical solution of the PDF via Monte Carlo schemes. (2) Development of algebraic turbulence closures for high speed reacting flows. (3) Implementation of the models developed in (2) in the computer code LARCK. (4) Applications of the LES-PDF methodology for flows of interest to NASA LaRC. (5) Utilization of DNS for model assessments. We do not have significantly new results since our last report pertaining to item (2) to present here. We have made significant progress in regard to tasks in item (3). However, since a thesis is under preparation to be submitted to NASA LaRC within the next month, this item is not discussed in the present report. Item (4) is relatively new and no results are presently available to present. The major thrust of this report is to provide a detailed descriptions of our achievements under items (1) and (5).

2 The Filtered Density Function for LES of Chemically Reacting Flows

The prediction of turbulent flows has been the focus of extensive research due to its importance in practical engineering applications. In past decades the analyst has had three main tools in the simulation of turbulent flows. The traditional approach in prediction of flows for engineering applications has been to consider the Reynolds averaged Navier-Stokes (RANS) equations. In RANS computation, the equations of motion for time averaged transport variables are solved. As a consequence of the averaging procedure, models must be provided to account for the effects of the turbulence on the mean flow. Alternatively, direct numerical simulation (DNS), in which all scales of the flow are resolved, offers the advantage that the

turbulence is explicitly calculated rather than modeled. Due to the very fine grids required in such model free simulations, DNS is typically restricted to very simple flows making its application to engineering problems impractical. Large eddy simulation (LES) offers a compromise between DNS and RANS computation (Givi, 1989; Libby and Williams, 1994; Givi, 1994; Rogallo and Moin, 1984; Lumley, 1990; Galperin and Orszag, 1993; Voke and Collins, 1983; Reynolds, 1990; Oran and Boris, 1991). In LES, local volume averaging is utilized to obtain a smoothed solution which can be captured on reasonable grids. In contrast to RANS computation in which all time (and implicitly length) scales must be modeled, only the smallest scales of the turbulent flow require closure, while the larger turbulent flow structure is resolved.

Over the past thirty years since the early work of Smagorinsky (1963) there has been relatively little effort, compared to that in RANS calculations, to make full use of LES for engineering applications. The most prominent model has been the Smagorinsky eddy viscosity based closure which relates the unknown subgrid scale (SGS) Reynolds stresses to the local large scale rate of flow strain (Lilly, 1965; Lilly, 1967). This viscosity is aimed to provide the role of mimicking the dissipative behavior of the unresolved small scales. The extensions to "dynamic" models (Germano, 1992; Germano *et al.*, 1991; Moin *et al.*, 1991; Lilly, 1992) have shown some improvements. This is particularly the case in transitional flow simulations where the dynamic evolutions of the empirical model "constant" result in (somewhat) better predictions of the large scale flow features.

A survey of combustion literature reveals relatively little work in LES of chemically reacting turbulent flows (Givi, 1989; Pope, 1990). The primary stumbling block in this utilization is the lack of closures which can accurately account for the influence of unresolved subgrid scale (SGS) fluctuations (Madnia and Givi, 1993). It appears that Schumann (1989) was one of the first to conduct LES of a reacting flow. However, the assumption made in this work simply to neglect the contribution of the SGS scalar fluctuations to the filtered reaction rate is debatable. The importance of such fluctuations is well recognized in RANS computation of reacting flows in both combustion (Libby and Williams, 1980; Libby and Williams, 1994; Jones and Whitelaw, 1984; Jones, 1994) and chemical engineering (Brodkey, 1975; Toor, 1975; Hill, 1976; Brodkey, 1981) problems. Therefore, it is natural to believe that these fluctuations will also have a significant influence in LES.

Modeling of scalar fluctuations in RANS has been the subject of intense investigations since the pioneering work of Toor (1962). The aim of statistical moment methods is to provide a closure for these correlations in terms of the mean flow variables. Eddy break up type closures (Spalding, 1977), which were popular in the 1970's, have achieved only a limited degree of success. Because of the lack of models with universal applicability to accurately predict the scalar correlations in turbulent reactive flows, simulations involving turbulent combustion are often met with a degree of skepticism. Another approach which has proven particularly useful is based on the probability density function (PDF) or the joint PDF of scalar quantities (O'Brien, 1980; Pope, 1985; Dopazo, 1994). This approach offers the advantage that all the statistical information pertaining to the scalar field is embedded within the PDF. Because of this feature, PDF methods have been widely used in RANS for a variety of reacting systems (see Dopazo (1994) for a recent review). The systematic approach for determining the PDF is by means of solving the transport equation governing its evolution (Lundgren, 1967; Lundgren, 1972; O'Brien, 1980). In this equation the effects of chemical reaction appear in a closed form. However, modeling is needed to account for transport of the PDF in the composition domain of the random variables. In addition, there is an extra dimensionality associated with the composition domain which must be treated. An alternative approach is based on *assumed* PDF in which the PDF is parameterized *a priori* in terms of its lower (usually the first two) moments. Obviously, this method is *ad hoc* but it offers more flexibility than the first approach. Presently the use of assumed methods in RANS is justified in cases where there is strong evidence that the PDF adopts a particular distribution (Rhodes, 1975; Jones and Priddin, 1978; Janicka and Kollmann, 1979; Lockwood and Moneib, 1980; Bockhorn, 1988; Priddin, 1991; Madnia *et al.*, 1992; Frankel *et al.*, 1993b; Miller *et al.*, 1993).

In an attempt to account for the effects of the subgrid scales on the filtered reaction rate, the eddy break up concept has been adopted for use in LES (Fureby and Lofstrom, 1994; Garrick, 1995). As in the case of RANS computation, such closures have achieved only a limited degree of success. Despite the demonstrated capabilities of PDF methods in RANS, their use in LES is limited (Givi, 1989; Madnia and Givi, 1993). The first application of PDF-LES is due to Madnia and Givi (Madnia and Givi, 1993) in which the *Pearson* family of PDF's are used for modeling of the SGS reactant conversion rate in homogeneous flows under chemical equilibrium conditions. This procedure was also used later by Cook and Riley (Cook and Riley, 1994) for LES of a similar flow. The extension of assumed PDF model for LES

of nonequilibrium reacting shear flows is reported by Frankel *et al.* (Frankel *et al.*, 1993a; Frankel, 1993). While the generated results are encouraging, they do reveal the need for more systematic schemes. Most of the drawbacks of these schemes can be overcome by considering the solution to the equation governing the evolution of the PDF. Because of the added dimensionality of the PDF transport equation, its solution by conventional numerical methods is possible in only the simplest of cases (Janicka *et al.*, 1979). An analysis performed by Pope (1981) suggests that the solution of the joint velocity-scalar PDF by finite difference methods is impractical for more than three scalars. However, the Lagrangian "Monte Carlo" scheme (Pope, 1985) can be used for this purpose. While PDF transport methods have enjoyed significant development in the past decade, no attempt has ever been made in its utilization for LES.

In this work, the Lagrangian PDF methodology is utilized as a means of providing the scalar SGS correlations for chemically reactive flows under nonequilibrium conditions. The Lagrangian approach, which has proven extremely effective in Reynolds averaging procedures, offers an attractive means of predicting the evolution of the "filtered density function" (FDF), which is essentially the PDF of SGS variables. In this paper we demonstrate its enormous potential for LES of turbulent combustion.

3 Mathematical Formulation

3.1 Governing transport equations

In the present treatment, incompressible flows undergoing isothermal reaction are considered. The restrictions regarding variable density due to exothermicity require attention, however they do not significantly alter the fundamental analysis and are readily removed. In the computational treatment of such flows, the primary independent transport variables are: the velocity vector u_i $(i = 1, 2, 3)$, the pressure p, and the species mass fractions ϕ_α $(\alpha = 1, 2, \ldots, N_s)$. The conservation equations governing these variables are given by:

Continuity:

$$\frac{\partial u_i}{\partial x_i} = 0 \tag{1}$$

Conservation of momentum:

$$\frac{\partial u_j}{\partial t} + \frac{\partial u_i u_j}{\partial x_i} = -\frac{\partial p}{\partial x_j} + \frac{\partial \tau_{ij}}{\partial x_i} \tag{2}$$

Conservation of chemical species:

$$\frac{\partial \phi_\alpha}{\partial t} + \frac{\partial u_i \phi_\alpha}{\partial x_i} = -\frac{\partial J_i^\alpha}{\partial x_i} + \dot{\omega}_\alpha. \tag{3}$$

The viscous stress tensor τ_{ij} and mass flux J_i^α of chemical species α are given by:

$$\tau_{ij} = \mu \left(\frac{\partial u_i}{\partial x_j} + \frac{\partial u_j}{\partial x_i} \right) \tag{4}$$

$$J_i^\alpha = -\Gamma \frac{\partial \phi_\alpha}{\partial x_i}. \tag{5}$$

where μ is the molecular viscosity, $\Gamma = \mu/Sc$ and Sc is the Schmidt number. The transport equations given above provide a complete description of the reactive system. However, the variations in length and time scales would require computational resolutions which are too prohibitive for even the fastest of today's supercomputers(Zang *et al.*, 1989). In RANS, solutions of the time averaged transport equations are attempted. In LES, instead of averaging over all time (and implicitly length) scales, the transport pertaining to the larger, energy containing eddies are considered. This allows resolution of the lower frequency turbulent structures. Operationally, this involves the use of a local "spatial filter" (Aldama, 1990):

$$\bar{f}(\mathbf{x}, t) = \int_{-\infty}^{+\infty} f(\mathbf{x}', t) G(\mathbf{x}' - \mathbf{x}) d\mathbf{x}' \tag{6}$$

where $\bar{f}$ represents the filtered value of the transport variable f; $G(\mathbf{x})$ denotes the filter and $f' = f - \overline{f}$ denotes the fluctuations from the filtered value. With the application of the filtering operation to the governing transport equations, we obtain:

$$\frac{\partial \overline{u}_i}{\partial x_i} = 0 \tag{7}$$

$$\frac{\partial \overline{u}_j}{\partial t} + \frac{\partial \overline{u}_i \overline{u}_j}{\partial x_i} = -\frac{\partial \overline{p}}{\partial x_j} + \frac{\partial \overline{\tau}_{ij}}{\partial x_i} - \frac{\partial T_{ij}}{\partial x_i} \tag{8}$$

$$\frac{\partial \overline{\phi}_\alpha}{\partial t} + \frac{\partial \overline{u}_i \overline{\phi}_\alpha}{\partial x_i} = -\frac{\partial \overline{J}_i^\alpha}{\partial x_i} - \frac{\partial M_i^\alpha}{\partial x_i} + \overline{\dot{\omega}}_\alpha \tag{9}$$

where $T_{ij} = \overline{u_i u_j} - \overline{u}_i \overline{u}_j$, $M_i^\alpha = \overline{u_i \phi_\alpha} - \overline{u}_i \overline{\phi}_\alpha$ and $\overline{\dot{\omega}}_\alpha$ are unclosed terms.

3.2 Modeling of unresolved scales

The quantities T_{ij} and M_i^α introduced in the previous section represent the effects of the small scale turbulence on the larger scales. A model must be introduced to properly account for these effects. The use of gradient diffusion models, particularly the one introduced by Smagorinsky (1963), have enjoyed a reasonable amount of success. While more sophisticated two-equation models, Reynolds stress models and Algebraic Reynolds stress models have undergone significant development for RANS computation, the turbulence models developed for LES are considerably less complicated. This is at least partially due to the fact that in LES less of the turbulence is modeled (and more is resolved) than in RANS computation. The Smagorinsky model is a gradient diffusion model which takes on the form:

$$T_{ij} - (\delta_{ij}/3) T_{kk} = -2\mu_t \overline{S}_{ij} \tag{10}$$

where $\overline{S}_{ij}$ is the large scale strain rate tensor and

$$\mu_t = C_s \Delta_G^2 \sqrt{\overline{S}_{ij} \overline{S}_{ij}}. \tag{11}$$

The dynamical interaction between resolved and SGS fields in isotropic turbulence was studied in detail by Kerr *et al.* (1996). Their results at different Reynolds number show that there is a strong correlation between large scale energy and SGS dissipation. This correlation implies that SGS dissipation is most effective at those physical locations which are rich in the large-scale energy. They conclude that at least in isotropic turbulence large-scale energy is a good indicator of nonlinear SGS interactions. Based on these observations we propose

to model the eddy viscosity with the following (MKEV) model:

$$\mu_t = C_k \Delta_G \sqrt{|\overline{u}_i \overline{u}_i - \widehat{\overline{u}}_i \widehat{\overline{u}}_i|}. \tag{12}$$

where the carat denotes the filter at the secondary level which has a characteristic size larger than that of grid level filter, and Δ_G is the filter width. We have found reasonable results for $\widehat{\Delta}_G/\Delta_G = 3$ where $\widehat{\Delta}_G$ is the characteristic size of the secondary level filter. Note that the observations by Kerr *et al.* were for homogeneous flows and the model has been presented so as to satisfy Galilean invariance for inhomogeneous flows. For homogeneous isotropic flows $\widehat{\overline{u}}_i \to 0$ as $\widehat{\Delta}_G \to \infty$. This model is essentially a modified version of that proposed by Bardina *et al.* (1983), which utilize equal sizes for the grid and secondary filters.

A similar model may be used to close the subgrid mass fluxes:

$$M_i^\alpha = -\Gamma_t \frac{\partial \overline{\phi}_\alpha}{\partial x_i} \tag{13}$$

where $\Gamma_t = \mu_t / Sc_t$, and Sc_t is the turbulent Schmidt number.

Thus far we have not yet addressed the issue of how to deal with scalar correlations in the filtered chemical source terms. For second order isothermal reactions, the correlation $\overline{\phi_\alpha \phi_\beta}$ must be properly modeled in order to correctly account for its effects on the larger scales. The SGS unmixedness ($\tau_{\alpha\beta} = \overline{\phi_\alpha \phi_\beta} - \overline{\phi}_\alpha \overline{\phi}_\beta$) represents the effect of SGS scalar-scalar corelation on the filtered chemical source terms. In RANS calculations the importance of the unmixedness term has long been recognized. In LES, the importance of this term has not been well appraised. While the SGS stress and flux terms discussed in this section are of a *convective* nature and can be reasonably well modeled by a *diffusive* process, the same cannot be said for the unclosed terms in the species production rates. Because the physical mechanism of the SGS stresses and fluxes is inherently different from the scalar correlations in the chemical source terms, it is expected that the models will differ. In fact, when eddy viscosity concepts are extended to treat chemical source terms, the resulting models ("eddy break up models") perform mediocre at best. The focus of the following sections is to discuss how the LES-PDF methodology is used to overcome the closure problem of the chemical source terms and to develop robust numerical methods for the simulation of turbulent reactive flows.

3.3 The filtered density function (FDF)

The most effective means of dealing with the statistical closure problem is to consider the joint PDF of the transport variables. For the purpose of simplicity, here we first consider the scalar array $\boldsymbol{\phi}(\mathbf{x},t)$ only; treatment of joint velocity-scalars follow a similar procedure. For this array, the "filtered density function" (FDF), denoted by P_L, is defined as (Pope, 1990):

$$P_L(\boldsymbol{\psi};\mathbf{x},t) = \int_{-\infty}^{+\infty} \varrho\left[\boldsymbol{\psi},\boldsymbol{\phi}(\mathbf{x}',t)\right] G(\mathbf{x}'-\mathbf{x})d\mathbf{x}' \tag{14}$$

$$\varrho\left[\boldsymbol{\psi},\boldsymbol{\phi}(\mathbf{x},t)\right] = \delta[\boldsymbol{\psi}-\boldsymbol{\phi}(\mathbf{x},t)] \equiv \prod_{\alpha=1}^{N_s} \delta[\psi_\alpha - \phi_\alpha(\mathbf{x},t)] \tag{15}$$

where δ denotes the delta function and $\boldsymbol{\psi}$ denotes the "composition domain" of the scalar array. The term $\varrho[\boldsymbol{\phi}-\boldsymbol{\psi}(\mathbf{x},t)]$ is the "fine-grained" density (O'Brien, 1980; Pope, 1985), and Eq. (15) implies that the FDF is the *spatially filtered* value of the fine-grained density. The FDF in this way, was first defined formally by Pope (Pope, 1990) and it has been discussed by others (Madnia and Givi, 1993; Gao and O'Brien, 1993). However, it has yet to be systematically used in actual LES.

Evaluations of spatial filtered values of the transport variable are achieved by integrating the FDF, exactly similar to that in PDF. For example, for the function $\mathcal{A}(\boldsymbol{\phi})$, the filtered (desired LES) value is:

$$\overline{\mathcal{A}}(\mathbf{x},t) = \int_{-\infty}^{+\infty} \mathcal{A}(\mathbf{x}',t)G(\mathbf{x}'-\mathbf{x})d\mathbf{x}' \equiv \int_{-\infty}^{+\infty} \mathcal{A}(\boldsymbol{\psi})P_L(\boldsymbol{\psi};\mathbf{x},t)d\boldsymbol{\psi}. \tag{16}$$

More generally, the conditionally filtered value of any function $\mathcal{A}(\mathbf{x},t)$ may be evaluated by integration over the whole of the compositional domain:

$$\langle\mathcal{A}(\mathbf{x},t)|\boldsymbol{\psi}\rangle\, P_L(\boldsymbol{\psi};\mathbf{x},t) = \int_{-\infty}^{+\infty} \mathcal{A}(\mathbf{x}',t)\delta[\boldsymbol{\phi}(\mathbf{x}',t)-\boldsymbol{\psi}]G(\mathbf{x}'-\mathbf{x})d\mathbf{x}'. \tag{17}$$

The unconditional average may be obtained by:

$$\overline{\mathcal{A}}(\mathbf{x},t) = \int_{-\infty}^{+\infty} \langle\mathcal{A}(\mathbf{x},t)|\boldsymbol{\psi}\rangle\, P_L(\boldsymbol{\psi};\mathbf{x},t)d\boldsymbol{\psi}. \tag{18}$$

If the variable $\mathcal{A}$ is completely determined by the compositional variable $\boldsymbol{\psi}$, then this last expression reduces to Eq. (16).

3.4 FDF transport equation for reactive scalars

The equation governing the transport of the scalar PDF may be derived by averaging the evolution equation of the fine-grained PDF (Lundgren, 1967; Lundgren, 1972; Stratonovich, 1963; Pope, 1976). In an analogous manner, the FDF transport equation may be arrived at by *spatially filtering* the same fine-grained transport equation. Alternately, Pope (1985) suggested an approach in which two independent expressions for $\langle DQ/Dt \rangle$ are equated. The same methodology may be applied to derive the evolution equation of the FDF. Another procedure, based upon Eqs. (14) and (17), is presented here.

Differentiation of Eq. (14) with respect to time yields:

$$\frac{\partial P_L(\boldsymbol{\psi};\mathbf{x},t)}{\partial t} = -\int_{-\infty}^{\infty} \frac{\partial \phi_\alpha}{\partial t} \frac{\partial \delta(\boldsymbol{\phi}(\mathbf{x}',t)-\boldsymbol{\psi})}{\partial \psi_\alpha} G(\mathbf{x}'-\mathbf{x})d\mathbf{x}' =$$

$$-\frac{\partial}{\partial \psi_\alpha}\int_{-\infty}^{\infty} \frac{\partial \phi_\alpha}{\partial t}\delta(\boldsymbol{\phi}(\mathbf{x}',t)-\boldsymbol{\psi})G(\mathbf{x}'-\mathbf{x})d\mathbf{x}'. \tag{19}$$

This expression can be combined with Eq. (17) to obtain:

$$\frac{\partial P_L(\boldsymbol{\psi};\mathbf{x},t)}{\partial t} = -\frac{\partial}{\partial \psi_\alpha}\left[\left\langle \frac{\partial \phi_\alpha}{\partial t}|\boldsymbol{\psi}\right\rangle P_L(\boldsymbol{\psi};\mathbf{x},t)\right]. \tag{20}$$

Utilization of Eq. (3) into this last expression yields:

$$\frac{\partial P_L(\boldsymbol{\psi};\mathbf{x},t)}{\partial t} = \frac{\partial}{\partial \psi_\alpha}\left\{\left[\left\langle \frac{\partial u_i \phi_\alpha}{\partial x_i}|\boldsymbol{\psi}\right\rangle + \left\langle \frac{\partial J_i^\alpha}{\partial x_i}|\boldsymbol{\psi}\right\rangle - \langle \omega_\alpha(\boldsymbol{\phi})|\boldsymbol{\psi}\rangle\right] P_L(\boldsymbol{\psi};\mathbf{x},t)\right\}. \tag{21}$$

The convective term may be decomposed into large and small scale contributions:

$$\frac{\partial}{\partial \boldsymbol{\psi}_\alpha}\left[\left\langle \frac{\partial u_i \phi_\alpha}{\partial x_i}|\boldsymbol{\psi}\right\rangle P_L(\boldsymbol{\psi};\mathbf{x},t)\right] =$$

$$\frac{\partial}{\partial \boldsymbol{\psi}_\alpha}\left\{\left[\overline{u}_i\left\langle \frac{\partial \phi_\alpha}{\partial x_i}|\boldsymbol{\psi}\right\rangle + \left(\left\langle u_i \frac{\partial \phi_\alpha}{\partial x_i}|\boldsymbol{\psi}\right\rangle - \overline{u}_i\left\langle \frac{\partial \phi_\alpha}{\partial x_i}|\boldsymbol{\psi}\right\rangle\right)\right] P_L(\boldsymbol{\psi};\mathbf{x},t)\right\}. \tag{22}$$

A similar manipulation to that used to obtain Eq. (19) can be used to recast the large scale convective term in a more familiar form:

$$\frac{\partial}{\partial \psi_\alpha}\left[\overline{u}_i \left\langle \frac{\partial \phi_\alpha}{\partial x_i} | \boldsymbol{\psi} \right\rangle P_L(\boldsymbol{\psi}; \mathbf{x}, t)\right] = -\frac{\partial \overline{u}_i P_L(\boldsymbol{\psi}; \mathbf{x}, t)}{\partial x_i}. \tag{23}$$

The FDF transport equation then takes on the form:

$$\frac{\partial P_L}{\partial t} + \frac{\partial \overline{u}_i P_L}{\partial x_i} = \frac{\partial}{\partial \psi_\alpha}\left\{\left[\left\langle u_i \frac{\partial \phi_\alpha}{\partial x_i} | \boldsymbol{\psi} \right\rangle - \overline{u}_i \left\langle \frac{\partial \phi_\alpha}{\partial x_i} | \boldsymbol{\psi} \right\rangle\right] P_L\right\} + \frac{\partial}{\partial \psi_\alpha}\left[\left\langle \frac{\partial J_i^\alpha}{\partial x_i} | \boldsymbol{\psi} \right\rangle P_L\right] - \frac{\partial [\omega_\alpha(\boldsymbol{\psi}) P_L]}{\partial \psi_\alpha}. \tag{24}$$

The first two terms on the left hand side of the equation represent the large scale convection of the FDF in physical space and appear in closed form. The first term on the right hand side denotes the effects of unresolved small scale convection of the FDF in physical space and requires closure. The second term on the right hand side represents molecular mixing and diffusion and requires modeling. In general, the mixing term tends to homogenize the fluid and hence lowers the scalar variance. The last term on the right hand side is due to chemical reaction which is in a closed form. The major advantage of PDF methods is that the scalar correlations in the filtered reaction rate do not need to be modeled. Instead, the effects of reaction are exactly accounted for without approximation. Note that the last two terms contain derivatives in compositional space rather than physical space. This is reflected by the fact that the processes of mixing and chemical reaction serve to change the compositional makeup of the mixture rather than to provide a mechanism for transport in physical space. Effectively, the last two bracketed terms on the right hand side are fluxes in the compositional domain.

3.5 Modeled FDF transport equation

While no modeling is required to account for the reaction source term in Eq. (24), the small scale convective term must be modeled to account for the effects of the turbulent transport of the FDF in the physical domain, and a model must be presented for the conditional expected diffusion in the molecular mixing term to account for transport in the domain of the compositional variables.

A gradient diffusion model of the form

$$\frac{\partial}{\partial \psi_\alpha}\left\{\left[\left\langle u_i \frac{\partial \phi_\alpha}{\partial x_i}|\psi\right\rangle - \overline{u}_i\left\langle \frac{\partial \phi_\alpha}{\partial x_i}|\psi\right\rangle\right] P_L\right\} = \frac{\partial}{\partial x_i}\Gamma_t \frac{\partial P_L}{\partial x_i} \tag{25}$$

is adopted to account for the small scale convective effects. This equation may be integrated to generate moment expression for the subgrid moments. For example, the first subgrid moment of Eq. (25) is given by:

$$-\left[\overline{u_i \frac{\partial \phi_\alpha}{\partial x_i}} - \overline{u}_i \overline{\frac{\partial \phi_\alpha}{\partial x_i}}\right] = \frac{\partial}{\partial x_i}\Gamma_t \frac{\partial \overline{\phi}_\alpha}{\partial x_i}. \tag{26}$$

Similar expressions may be derived for the higher order subgrid moments. One must be careful in the integration procedure to obtain Eq. (26) in the case where the spatial filter varies with respect to the spatial coordinate. This is due to the fact that for nonuniform filters, the filter and derivative operators do not commute.

Modeling of the molecular mixing term has been the focus of intense investigation (Pope, 1985). Most of the models currently in use are based on the family of Coalescence/Dispersion (C/D) closures (Curl, 1963; Dopazo and O'Brien, 1976; Pope, 1976; Janicka *et al.*, 1979; Pope, 1979; Pope, 1982; Kosály and Givi, 1987; McMurtry and Givi, 1989). Our previous investigations (Kosály and Givi, 1987; McMurtry and Givi, 1989) indicate that in homogeneous turbulence the predicted results are sensitive to the choice of the mixing model. However, it is anticipated that in the context of inhomogeneous LES, different members of C/D models behave very similarly, particularly for the lower order moments. Amongst these members the one which is the most convenient to use is the linear mean square estimation (LMSE) model (O'Brien, 1980; Dopazo and O'Brien, 1976). In the adaptation of this model for LES, the value of the transport quantity relaxes to the "spatially filtered" value at the point of interest. For a scalar governed by Fickian diffusion, the molecular mixing within the subgrid is modeled as:

$$\frac{\partial}{\partial \psi_\alpha}\left[\left\langle -\frac{\partial}{\partial x_i}\left(\Gamma \frac{\partial \phi_\alpha}{\partial x_i}\right)\ |\psi\right\rangle P_L\right] = \frac{\partial}{\partial x_i}\left(\Gamma \frac{\partial P_L}{\partial x_i}\right) + \frac{\partial}{\partial \psi_\alpha}\left[\frac{C_\phi \Omega_m}{2}(\psi_\alpha - \overline{\phi}_\alpha)P_L\right] \tag{27}$$

where Ω_m is the frequency of mixing within the subgrid and can be related to the subgrid diffusion coefficient and the filter length: $\Omega_m = C_\Omega(\Gamma + \Gamma_t)/\Delta_G^2$.

With the closures given by Eqs. (25) and (27), the final modeled FDF transport equation is given by:

$$\frac{\partial P_L}{\partial t} + \frac{\partial[\overline{u}_i P_L]}{\partial x_i} = \frac{\partial}{\partial x_i}(\Gamma + \Gamma_t)\frac{\partial P_L}{\partial x_i} + \frac{\partial}{\partial \psi_\alpha}\left[\frac{C_\phi \Omega_m}{2}(\psi_\alpha - \overline{\phi}_\alpha)P_L\right] - \frac{\partial[\omega_\alpha(\boldsymbol{\psi})P_L]}{\partial \psi_\alpha}. \tag{28}$$

3.6 Consistency between FDF and moment closure approaches

The modeled evolution equation for the FDF, Eq. (28), may be integrated to obtain transport equations for the moments. While the derivations to this point have been completely general with regard to variable spatial filters, the restriction of uniform filters is invoked for this section. With a few notable exceptions, nearly all SGS modeling has been developed for uniform filters.

In the case that the spatial filter is not a function of space the convective effects may be taken into account via the decomposition:

$$\langle u_i|\boldsymbol{\psi}\rangle\, P_L = \overline{u}_i P_L + [\langle u_i|\boldsymbol{\psi}\rangle - \overline{u}_i]P_L = \overline{u}_i\overline{\varrho} + [\overline{u_i\varrho} - \overline{u}_i\overline{\varrho}]. \tag{29}$$

This result is easily derived by imposing the restriction of constant filter size on the decomposition given by Eq. (22). The attractiveness of the decomposition given by Eq. (29) is that upon integration, it yields results identical to those in conventional LES. For example, the first moment of Eq. (29) is:

$$\overline{u_i\phi_\alpha} = \overline{u}_i\overline{\phi}_\alpha + [\overline{u_i\phi_\alpha} - \overline{u}_i\overline{\phi}_\alpha]. \tag{30}$$

The term in brackets in Eq. (30) is the generalized scalar flux in the format defined by Germano (1992). Thus, if a gradient diffusion model of the form

$$[\langle u_i|\boldsymbol{\psi}\rangle - \overline{u}_i]P_L = -\Gamma_t\frac{\partial P_L}{\partial x_i} \tag{31}$$

is adopted, the first moment of the FDF satisfies:

$$[\overline{u_i\phi_\alpha} - \overline{u}_i\overline{\phi}_\alpha] = -\Gamma_t\frac{\partial\overline{\phi}_\alpha}{\partial x_i}. \tag{32}$$

This is similar to the Smagorinsky type closure (Lilly, 1965; Lilly, 1967) as used in conventional LES (with or without the dynamic (Germano, 1992; Germano *et al.*, 1991) model). Of course, this similarity does not imply that the FDF is "equivalent" to the Smagorinsky closure. Although the two closures yield similar results for the "first subgrid" moment of a "non-reacting" scalar, the FDF includes all the higher moments of all the reacting scalar variables.

For uniform filters, the conditional expected diffusion can be decomposed into diffusive and dissipative parts:

$$\frac{\partial}{\partial\psi_\alpha}\left[\left\langle -\frac{\partial}{\partial x_i}\left(\Gamma\frac{\partial\phi_\alpha}{\partial x_i}\right)\ |\boldsymbol{\psi}\right\rangle P_L\right] = \frac{\partial}{\partial x_i}\left(\Gamma\frac{\partial P_L}{\partial x_i}\right) - \frac{\partial^2}{\partial\psi_\alpha\partial\psi_\alpha}\left[\left\langle\Gamma\frac{\partial\phi_\alpha}{\partial x_i}\frac{\partial\phi_\alpha}{\partial x_i}|\boldsymbol{\psi}\right\rangle P_L\right]. \quad (33)$$

This isolates the effect of scalar dissipation for which LMSE provides a closure:

$$\frac{\partial^2}{\partial\psi_\alpha\partial\psi_\alpha}\left[\left\langle\Gamma\frac{\partial\phi_\alpha}{\partial x_i}\frac{\partial\phi_\alpha}{\partial x_i}|\boldsymbol{\psi}\right\rangle P_L\right] = -\frac{\partial}{\partial\psi_\alpha}\left[\frac{C_\phi\Omega_m}{2}(\psi_\alpha - \overline{\phi}_\alpha)P_L\right]. \quad (34)$$

This again, yields results consistent with conventional LES for the first two subgrid moments. While the first moment of Eq. (34) yields a trivial result (molecular mixing has no effect on the mean), its second moment generates an expression for the dissipation:

$$-2\Gamma\overline{\frac{\partial\phi_\alpha}{\partial x_i}\frac{\partial\phi_\alpha}{\partial x_i}} = \frac{C_\phi\Omega_m}{2}(\overline{\phi_\alpha^2} - \overline{\phi_\alpha}^2). \quad (35)$$

The modeled FDF transport equation, Eq. (28), may be integrated to obtain transport equations for all the desired moments. For instance, with the assumption of a uniform filter width, the equation for the first subgrid moment is given by:

$$\frac{\partial\overline{\phi}_\alpha}{\partial t} + \frac{\partial\overline{u}_i\overline{\phi}_\alpha}{\partial x_i} = \frac{\partial}{\partial x_i}(\Gamma + \Gamma_t)\frac{\partial\overline{\phi}_\alpha}{\partial x_i} + \overline{\dot{\omega}}_\alpha. \quad (36)$$

Similarly, the transport equations for higher order moments may be derived:

$$\frac{\partial\sigma_\alpha^2}{\partial t} + \frac{\partial\overline{u}_i\sigma_\alpha^2}{\partial x_i} = \frac{\partial}{\partial x_i}(\Gamma + \Gamma_t)\frac{\partial\sigma_\alpha^2}{\partial x_i} - C_\phi\Omega_m\sigma_\alpha^2 + 2(\Gamma + \Gamma_t)\frac{\partial\overline{\phi}_\alpha}{\partial x_i}\frac{\partial\overline{\phi}_\alpha}{\partial x_i} + 2(\overline{\phi_\alpha\dot{\omega}_\alpha} - \overline{\phi}_\alpha\overline{\dot{\omega}}_\alpha) \quad (37)$$

where $\sigma_\alpha^2 = \overline{\phi_\alpha^2} - \overline{\phi_\alpha}^2$ is the generalized subgrid variance of chemical species ϕ_α. It should

be noted that the quantity σ_α^2 is more useful in LES than the quantity $\overline{\phi'_\alpha \phi'_\alpha}$ as the former term represents the entire deviation between the subgrid and resolved scales while the latter term does not account for cross and Leonard stresses. Under the restrictions of no chemical reaction, it is clear that direct solution of the moment equations (36) - (37) yields the exact same information for the first two moments as those generated by the solution of the modeled FDF transport equation. This consistency is exploited by comparing the solution to the moment equations and the FDF under non-reacting conditions. This allows verification that the numerical solution to the FDF is accurately capturing the effects of convection, mixing and diffusion.

While it has been shown that consistent models for turbulent transport and molecular mixing (i.e. dissipation) may be derived, no such consistency condition exists for the reaction source term. This is a consequence of the simple fact that no model for reaction is required in the FDF treatment, and hence the analogous moment closure does not exist. Under chemically reactive conditions, the advantage of the FDF approach is obviated; no model is required to treat the nonlinear (and arbitrarily complicated) chemical source terms, while the moment equations require such a model. This is particularly important as at the present time no generally applicable reaction model has ever been proposed for use in LES.

3.7 The Lagrangian approach, Langevin equation and equivalent systems

The solution of Eq. (24) provides all the statistical information pertaining to the scalar array $\phi(\mathbf{x}, t)$. This equation can be solved most effectively via the Monte Carlo scheme (Pope, 1981). Currently, two classes of Monte Carlo schemes are available: Eulerian and Lagrangian. In the Eulerian scheme, the PDF within the subgrid is represented by an ensemble of computational elements (or particles) at "fixed" grid points. These elements are transported in the "physical space" by the combined actions of large scale convection and diffusion (molecular and subgrid). In addition, transport in the "composition space" occurs due to chemical reaction and subgrid molecular mixing. In previous unpublished work, the Eulerian Monte Carlo method was tested for LES of a non-reacting shear flow. Expectedly, the results were not encouraging. The major difficulty with the Eulerian formulation lies in

the numerical implementation of the large scale convection. Due to "grid-based" nature of the scheme, excessive artificial diffusion is created which degrades the solution very notably. It is crucial to realize that the errors induced by this scheme are not due to the FDF formulation, but rather to the numerical implementation of the large scale convection.

A remedy for the problem noted above is to divorce from the Eulerian discretization and to invoke the Monte Carlo solver in a "grid free" Lagrangian manner. The Lagrangian procedure involves transport of the elements within the "whole" computational domain of interest. The advantages of this procedure in reducing the amount of numerical diffusion in DNS are well-recognized (Chorin, 1968; Chorin and Marsden, 1979; Leonard, 1980; Majda, 1988; Sarpkaya, 1989; Ghoniem, 1991; Gustafson and Sethian, 1991). The basis of the Lagrangian solution of the FDF transport equation relies upon the principle of *equivalent systems* (Pope, 1985; Pope, 1994). Two systems with different instantaneous behaviors may have identical statistics and satisfy the same FDF transport equation. In the Lagrangian solution procedure each of the particles obeys certain equations which govern its transport. It is important to recognize that these particles are not fluid elements. In fact, while fluid parcels follow smooth trajectories, it will be shown that the Monte Carlo particles follow trajectories which are continuous but <u>not</u> differentiable. The significance of these notional particles is that they are developed in such a way that they evolve with the same collective statistics as genuine fluid particles.

The Monte Carlo particles undergo motion in the physical space by convection due to the filtered mean flow velocity, and diffusion due to molecular and subgrid diffusivities. The general diffusion process may be represented in a stochastic manner by the Langevin equation (Pope, 1985; Risken, 1989; Gardiner, 1990; Gillespie, 1992):

$$dX_i(t) = D_i(\mathbf{X}(t), t)dt + B(\mathbf{X}(t), t)dW_i(t) \tag{38}$$

where X_i is the Lagrangian position of a stochastic particle. The entities D_i and B are known as the "drift" and "diffusion" coefficients, respectively, and W_i denotes the stochastic Wiener-Levy (Karlin and Taylor, 1981) process. This process is best understood by considering the

function $W_d(t_n)$ which changes at discrete time intervals:

$$W_d(t_n) = (\Delta t)^{1/2} \sum_{i=1}^{N} \xi_i, \tag{39}$$

where ξ_n $(n = 1, 2, \ldots, N)$ are N independent normalized Gaussian random variables and the time interval $[0, T]$ is divided into N equal subintervals of duration $\Delta t = T/N$. Consider the increment

$$\Delta W_d(t_{n-1}) = \xi_n (\Delta t)^{1/2}. \tag{40}$$

The Weiner process can be defined as Eqs. (39) - (40) in the limit $\Delta t \to 0$. Note that although the process is continuous, it is not differentiable since $\Delta W_d / \Delta t$ is undefined as Δt vanishes. For the system considered here, the stochastic particle locations are governed by the solution to the following stochastic differential equation:

$$dX_i(t) = \left[\overline{u}_i + \frac{\partial(\Gamma + \Gamma_t)}{\partial x_i} \right] dt + [2(\Gamma + \Gamma_t)]^{1/2} \, dW_i. \tag{41}$$

It must be emphasized that although the Langevin equation given by Eq. (41) is stochastic, Eq. (24) which governs the transport of the joint scalar PDF is deterministic.

While Eq. (41) dictates the spatial evolution of the FDF in the physical domain, the compositional makeup of the particle evolves simultaneously due to the actions of mixing and reaction. This is accomplished by solution to the differential equation

$$\frac{\partial \phi_\alpha^+}{\partial t} = \frac{\partial}{\partial \psi_\alpha} \left\langle \Gamma \frac{\partial \phi_\alpha}{\partial x_i} \frac{\partial \phi_\alpha}{\partial x_i} | \psi \right\rangle + \dot{\omega}_\alpha \tag{42}$$

where the quantity $\phi_\alpha^+ = \phi_\alpha(X_i(t), t)$ denotes the scalar value of the particle with the Lagrangian position vector X_i. With the introduction of the LMSE model, Eq. (42) takes on the form

$$\frac{\partial \phi_\alpha^+}{\partial t} = -\frac{1}{2} C_\phi \Omega_m (\psi_\alpha - \overline{\phi}_\alpha) + \dot{\omega}_\alpha. \tag{43}$$

Effectively, Eqs. (41) and (43) constitute an equivalent system with the same FDF that is governed by Eq. (28). It should be clear that while each individual particle evolves in the physical domain in a stochastic manner, the statistics of these particles which are used to evaluate the FDF evolve in a deterministic manner according to Eq. (28). The essence of

the Monte Carlo approach is not to directly simulate fluid particles and the associated FDF, but rather to *indirectly* determine the FDF by tracking notional particles which evolve with the identical statistics.

4 Numerical Approach

In the numerical implementation of the equivalent system discussed in the previous section, the FDF is represented by N_p Monte Carlo particles, each with a set of scalars $\phi_\alpha^{(n)}(\mathbf{X}^{(n)}(t),t)$ and Lagrangian position vector $\mathbf{X}^{(n)}$. Numerically, a splitting operation is used to treat the effects of physical transport, molecular mixing and chemical reaction separately. The simplest means of simulating Eq. (41) is via the Euler-Maruyamma approximation (Kloeden and Platen, 1995). This preserves the Markovian character of the diffusion process (Gillespie, 1992; Papoulis, 1965; Billingsly, 1979; Helfand, 1979; Schuss, 1980; Ross, 1996) and facilitates affordable computations. Operationally, this implies that if the time interval $[t_0, t \geq t_0]$ is divided into increments $t_0, t_1, t_2, \ldots t_i, t_{i+1}, \ldots t$ with $t_0 \leq t_1 \leq t_2 \leq \ldots t_i \leq t_{i+1} \leq \ldots t$, the "conditional" probability (for an event $\mathcal{A}$) obeys:

$$\text{Prob. } \{\mathcal{A}, t_n | t_1, t_2, \ldots t_{n_1}\} = \text{Prob. } \{\mathcal{A}, t_n | t_{n-1}\}. \tag{44}$$

Using the Euler-Maruyamma scheme, Eq. (41) takes on the discretized form:

$$X_i^n(t_{k+1}) = X_i^n(t_k) + D_i^n(t_k)\Delta t + B^n(t_k)(\Delta t)^{1/2}\xi_i^n(t_k) \tag{45}$$

where $D_i^n(t_k) = D_i(\mathbf{X}^{(n)}(t_k))$ and $B^n(t_k) = B(\mathbf{X}^{(n)}(t_k))$. Higher order numerical schemes for solving Eq. (41) are available (Kloeden and Platen, 1995), but one must be very cautious in actual simulations. It must be recognized that since in LES, the diffusion term in Eq. (38) strongly depends on the stochastic process $\mathbf{X}(t)$, the numerical scheme must preserve the Itô-Gikhman nature of the process. The coefficients D_i and B require the input of the filtered mean velocity and the diffusivity (molecular and subgrid eddy). These quantities are determined by conventional LES at standard finite difference grid points. Since the Monte Carlo particles are not restricted to the LES grid points, fourth order Lagrange polynomials are utilized to interpolate the desired quantities to the particle.

At each time step, the compositional values are subject to change due to subgrid molecular mixing and chemical reaction. Eq. (43) may be integrated numerically to simulate the effects of chemical reaction and dissipation simultaneously. Alternately, Eq. (43) may be treated in a time-split manner in which the effect of mixing and chemical reaction are treated separately. The advantage to this approach is that the compositional changes due to mixing may be expressed in an analytical manner. With the reaction term set to zero, Eq. (43) may be integrated analytically over a time step Δt to determine the change in composition due to molecular mixing. Consequentially each particle changes according to

$$(\phi_\alpha^n)^{mix} = \overline{\phi_\alpha^n} + (\phi_\alpha^n - \overline{\phi_\alpha^n}) \exp\left[-\frac{1}{2} C_\phi \Omega_m \Delta t\right] \tag{46}$$

at each time step. After this step, the particles undergo reaction. This is performed readily by sweeping over all the particles and determining the fine grain reaction rates ω_α^k and modifying the composition of each of the elements accordingly:

$$\phi_\alpha^n(t + \Delta t) = (\phi_\alpha^n)^{mix} + \omega_\alpha^n \Delta t. \tag{47}$$

The mixing procedure given by the LMSE model implementation Eq. (46) requires filtered value of the compositional vector $\overline{\phi}_\alpha$ as an input. The estimation of subgrid moments at a given point is conducted by consideration of particles within some volume centered at the point of interest. Effectively, this finite volume constitutes an "ensemble domain" (not to be confused with the "filter domain" characterized by the filter length Δ_G) in which the FDF is represented discretely by numerous stochastic particles. This is necessary as with probability one no particles will coincide with the point in question. Essentially, each particle represents a "fine grain value" and may be considered a single realization of the flow. Strictly speaking, it is not correct to literally equate a stochastic particle to a fluid sample, however the *collective statistics* they are used to generate are equivalent. In the present work, a simple box average is utilized as the ensemble domain at the finite difference grid nodes, and the fourth order Lagrangian interpolation procedure is used to interpolate these means to the particle positions. The size of the ensemble domain is an important issue and pertinent results are presented in a later section. Other methods used to calculate moments, such as those based on cubic splines, are not a subject of the current investigation. The numerical

scheme only relies upon the input of the filtered scalar value, and not its derivative, in the mixing model implementation. For this purpose the simple volume averaging procedure is sufficient.

The numerical procedure used to calculate the mean hydrodynamic transport variables utilizes a high order finite difference scheme as discussed by Carpenter (1990). This scheme is a variant of the well known MacCormack scheme in which fourth order compact differences are used to discretize the spatial derivatives. A second order symmetric predictor-corrector sequence is employed to achieve second order accuracy in time. The code solves the Navier Stokes equations in fully compressible form, however for the purposes of this paper all simulations are conducted at a low Mach number ($M = 0.3$) so as to minimize the effects of compressibility. The nature of the finite difference scheme is independent of the Monte Carlo method and alternative methods could be used in its place. One attractive feature of the Lagrangian scalar FDF Monte Carlo scheme is that it could be incorporated rather easily in the extensive stockpile of existing fluid dynamic codes.

5 Results

To demonstrate the effectiveness of the Monte Carlo FDF approach, two flow configurations are considered: (1) a temporally developing mixing layer and (2) a planar jet. For both configurations, a constant rate, non heat releasing chemical reaction of the type $A+B \rightarrow P$ is simulated. In this study, only two dimensional flows are considered. The fundamental theory is three dimensional and hence no special treatment is required to extend the simulations to 3 spatial dimensions.

The mixing layer configuration consists of two coflowing streams traveling at different velocities and merging at the trailing edge of a partition plate. Two reactants, A and B, are introduced into the high and the low speed streams, respectively. To expedite the formation of large scale vortices, low amplitude perturbations are initially superimposed on the mean flow. The flow field which develops in this setting is dominated by large scale coherent structures. In the spatial jet, reactant A is injected into the domain in the high speed stream while reactant B enters the domain in the lower speed coflow. Disturbances are introduced

at the inlet plane so as to facilitate the formation of large scale, energy containing eddies.

The assessment of the models is facilitated by direct comparison with DNS data. The resolution in DNS is dictated by the magnitudes of the physical parameters, with sufficient testing on the independency of the results to the number of grid points. The highest resolution in temporal shear layer simulations consists of 434×577 grid points. With this resolution, reliable DNS with a Reynolds number $Re = 2800$ and a Damköhler number $Da = 2$ (based on the velocity difference and the vorticity thickness at initial time) are possible. The length in streamwise direction is chosen to two times the wavelength of the most unstable mode given by linear stability theory. The scenario of the simulation showed the rollup of the spanwise vorticity, resulting in two spanwise rollers. Subsequently, pairing of these vortices was observed, reducing the number of vortices to one in later stages. The DNS of the spatially evolving jet was conducted on an evenly spaced grid with resolution of 601×301 grid points. With this resolution, accurate simulations up to $Re = 10,000$ and $Da = 2$ (based upon the jet diameter and centerline velocity) are possible. Large scale structures are generated by forcing of the cross-stream velocity at the inlet plane at a frequency corresponding to the most unstable mode as determined by linear stability theory. The velocity ratio of the high to low speed streams is 0.5. The computational domain extends 14 diameters downstream and is 7 diameters wide. In both flows, all the species (A, B, P) are assumed thermodynamically identical and the fluid is assumed to be calorically perfect. The value of the turbulent Schmidt number is set equal to 0.7 in all simulations.

The spatial filter Δ_G is set to twice the grid spacing for all simulations. The effect of the size of the "ensemble domain" is considered by comparing the results for FDF simulations performed using uniform box domains of dimension $\Delta x \times \Delta y$ and $2\Delta x \times 2\Delta y$ (in the present simulations the grid spacing $\Delta x = \Delta y$ is constant throughout the computational domain).

In order to assess the performance of the FDF methodology in predicting the scalar correlations in the chemical source terms, finite difference LES simulations are conducted in which the reaction rate is assumed to be a function of the mean species concentrations, thus neglecting any correlation due to the small scales. The convective turbulent transport terms are modeled in a "consistent" manner by utilizing the same eddy diffusivity, so any discrepancy can be attributed to the neglection of the scalar correlations in the mean reaction rates. In the degenerate case of an nonreactive scalar where the species conversion rate

is zero, the moment equation solved by the finite difference should yield the same results as those generated by solution to the FDF transport equation. Any deviation between the two must be attributed to differences in the numerical solution (i.e. Monte Carlo vs. finite difference).

5.1 Non-reacting simulations

In order to assess the validity of the convection, diffusion and dissipation numerical procedures, Monte Carlo FDF and "conventional" finite difference LES simulations were performed for a conserved scalar. As noted above, it is expected that the difference between the two approaches should be small, any discrepancy owing only to the different numerical methodologies.

In Fig. 1, results are presented of the LES of the non-reacting temporally developing mixing layer. The contour plots of the mean conserved scalar as obtained by (a) the FDF and (b) conventional LES approaches illustrate the consistency between the FDF and conventional LES methodologies. In fact, the Monte Carlo results are even more attractive due the Lagrangian nature of the solution procedure. Note the oscillations in the results provided by the conventional finite difference LES approach. While the finite difference method suffers from potential over and undershoots (which is controlled somewhat by clipping non physical values) in lower resolution LES simulations, there is no numerical mechanism to cause such errors in the Monte Carlo scheme (at least in the case of non-reacting scalars). Even with the addition of the subgrid diffusivity at this low resolution simulation, the conventional finite difference LES scheme is not capable of providing a solution free of numerical noise.

Figs. 2-3 show the variation of the mean (filtered) value and generalized variance of the conserved scalar, ϕ, across the shear layer. These statistics are gathered by averaging the data over the homogeneous (x) direction. This is represented by $[]_x$. Such statistics in the temporal simulations are the counterpart to Reynolds averaged quantities for spatially evolving flows. The most significant difference between the results obtained from FDF and conventional LES method are at the final time of the simulation ($t \approx 44$) when the merging of the two pairs of vortices is completed.

Figure 2(a) shows that the values of $[\overline{\phi}]_x$ evaluated from finite difference and Monte Carlo methods are indeed very close even when the FDF sample domain size is relatively large ($2\Delta x \times 2\Delta y$). The results for $[\overline{\phi^2}]_x$ (not shown) exhibit a similar behavior. The difference between FDF and LES is better observed in Figs. 2(b) and 2(c) where the variations of $[\sigma^2]_x = [\overline{\phi^2} - \overline{\phi}^2]_x$ with y for different mixing frequency constant (C_ϕ) are shown. As expected with increasing C_ϕ, the variance is significantly decreased. Nevertheless, the deviation between the variances calculated from FDF and LES methods is consistently insignificant. The numerical error due to the oscillatory behavior in the finite difference method is one of the reasons for the observed deviation between variances. However, the difference is mainly due to the finite size of the ensemble domain in the FDF calculation and is decreased as the size of ensemble domain for FDF calculation is decreased (Figs. 2(b) and 2(c)). Ideally, the best results from the Monte Carlo procedure are obtained when the size of sample domain is infinitely small and the number of particles within this domain is infinitely large. Since it is necessary to deal with a finite number of particles, a smaller domain size results in a fewer particles to construct the FDF with the consequence of higher statistical error. Alternately, a larger ensemble domain will result in a decrease in statistical error, however the consequence is an increase in spatial error which manifests itself in a diffusive type effect. The optimum size varies with many factors and can not in general be specified a priori. The results in Figs. 2(b) and 2(c) show that the variances evaluated from LES and FDF are reasonably well compared when the ensemble domain is $\Delta x \times \Delta y$. Therefore in most of the simulations this sample size is used. Other results shown below suggest that important statistical quantities such as the product thickness are not very sensitive to the sample size for calculation of FDF.

The sensitivity of the results to the number of particles and the time step of calculations are shown in Fig. 3. The time step may be especially important in the numerical integration of the stochastic Langevin equation and is decreased by decreasing the magnitude of CFL number. The value of $[\sigma^2]_x$ does not vary significantly with the particle number density as long as the particle density is not significantly low. This is observed in Fig. 3(a), where it is shown that even at the final time of the simulation $[\sigma^2]_x$ values calculated from particles are almost invariant with respect to particles number density. It is also shown in Fig. 3(b) that by decreasing the time step below that is required by stability considerations $[\sigma^2]_x$ remains invariant. The results for $[\overline{\phi}]_x$ (not shown) exhibits much less sensitivity to the initial number

of particles per cell and also to the time step.

FDF and finite difference simulations of the spatially evolving jet for a conserved scalar further support the observations noted in the case of the temporal shear layer. Fig. 4. are plots of the time averaged conserved scalar as a function of the cross-stream coordinate for several downstream positions. It is evident that the mean scalar is predicted in nearly identical form for the FDF and finite difference LES approaches. As in the case of the temporal shear layer, the results of the generalized variance exhibit a somewhat sensitive behavior to the size of the ensemble domain. This is confirmed by Fig. 5 which shows the variation of the time averaged generalized subgrid variance with the cross-stream direction for 2 downstream positions. The deviation between the FDF and finite difference LES approaches diminishes as the ensemble domain decreases.

5.2 Reactive simulations

The primary motivation for utilizing the FDF approach is that the scalar correlations appear in closed form thus avoiding the closure problem. The results of the previous section illustrate the equivalence of the FDF and moment closure approaches in the non-reactive case. This equivalence was exploited to demonstrate the effectiveness of the numerical scheme in predicting the combined effects of convection, diffusion and mixing. In this section the effects of nonequilibrium chemical reaction are considered. Under these conditions a consistently between the FDF and moment closure approaches no longer exists, and the full benefits of the FDF approach are be realized.

To conduct a resolution study, model free simulations at different resolutions are conducted. Temporal evolution of the vorticity and product thicknesses corresponding to these cases are shown in Fig. 6. In Fig. 6(a) it is observed that the calculated vorticity thickness for the simulation with 290×385 grid points is identical with that calculated based on 434×577 grid points. However, by decreasing the resolution to 38×49 the vorticity growth is decreased. Similar results are shown in Fig. 6(b) for the product thickness. Even at Da=2, the product thickness increases only very slightly when the resolution is decreased from 434×577 to 290×385. On the other hand, the predicted value of $\delta_{product}$ at low resolution (38×49)

is much higher than that obtained from high resolution simulations. Based on the results shown in Fig. 6, a resolution of 434×577 grid points is sufficient to resolve the hydrodynamic and scalar fields. The FDF and finite difference LES simulations are conducted on a 38×49 grid.

It is evident from the results shown in Fig. 6 that in LES the unresolved subgrid scales have a significant effect on the resolved scales. To show this and also to demonstrate the importance of τ_{AB} in LES, in Fig. 7 we consider the variation of the τ_{AB} (x-averaged) and its subpart, $R_{AB} = \overline{\phi'_A \phi'_B} - \overline{\phi'}_A \overline{\phi'}_B$ along y direction. Following Leonard (1974) and Germano (1986), τ_{AB} can be decomposed into subparts. Each of the terms in this decomposition is expected to constitute a significant part of the SGS unmixedness when a filter allowing overlap between resolved and unresolved scales is used, as for instance the Gaussian or the box filter. One of these subparts is R_{AB}, the "Reynolds" part. The results in Fig. 7 show that throughout the simulation R_{AB} is only a fraction of τ_{AB}. This suggests that the modeling of τ_{AB} in LES is more difficult than the modeling of the corresponding term in RANS calculations. In the previous LES of reacting flows τ_{AB} is either effectively ignored (Schumann, 1989; Liou *et al.*, 1994) or is modeled in an ad hoc basis (Fureby and Lofstrom, 1994).

In Fig. 8, the values of $\delta_{product}$ calculated from FDF method are compared to that obtained from filtered DNS data. In this calculation the Smagorinsky model (rather than the MKEV model) is used to evaluate the subgrid viscosity. The results in Fig. 8 show that regardless of the magnitude of the Smagorinsky constant (C_s), $\delta_{product}$ is not well predicted by FDF method even though the chemistry in this method is closed. The main reason is the inadequacy of the Smagorsinky model to predict the correct value of the subgrid viscosity in this transitional flow, which in turn results in a poor prediction of the mixing frequency. While the reaction is treated exactly in the FDF approach, the composition at which this reaction is evaluated at is effected by the selection of the mixing frequency. This points the importance of proper evaluation of the mixing frequency. It is well established that the Smagorinsky closure generates excessive damping on the resolved large scales in transitional regions and consequently wrong prediction of the growth rate of the shear layer. In the temporal shear layer C_s should be initially set to zero because the flow is laminar at this time. Gradually it should increase with the growth of the layer. As shown in Fig. 8, with choosing the Smagorinsky coefficient to be a linear function of time, the transitional nature of the flow is

well captured as well as the value of the subgrid viscosity, and in turn the mixing frequency. As a result, the values of $\delta_{product}$ calculated with $C_s \propto t$ compare favorably with the DNS values. Indeed, it is intriguing how well $\delta_{product}$ is predicted with this simple functional form for C_s. No attempt is made to propose this form of C_s for any flow, rather the intention is to emphasize the importance of the subgrid viscosity and particularly the associated mixing frequency in the FDF method and provides motivation to find a better model to calculate the subgrid viscosity.

Motivated to better predict the eddy viscosity, the MKEV model, Eq. (12), is adopted. The improved prediction of the subgrid viscosity has favorable consequences. First, it results in better prediction of the hydrodynamics which affects the mixing and reaction processes. Second, it yields better predictions of the subgrid diffusivity in the Langevin equation and the mixing frequency in the LMSE model. In Fig. 9 it is shown that the temporal evaluation of the vorticity thickness calculated from the above MKEV model is closer to that calculated from DNS than those calculated from Smagorinsky model. The Smagorinsky model with time varying (linear in time) coefficient better compares with the DNS than the Smagorinsky model with constant coefficient. Proper prediction of the subgrid viscosity has an even more significant effect on the chemistry as a result of the improvement of the mixing frequency. This is observed in Fig. 10(a) where $\delta_{product}$ as calculated by the FDF method is shown. It is observed that the FDF simulation compares favorably with the DNS over a range of Damkohler numbers. In Fig. 10(b) similar results are shown for LES calculations with models for the SGS stresses and scalar fluxes and no model for SGS unmixedness. Similar to that observed in Fig. 6(b), the LES values of $\delta_{product}$ are much higher than the corresponding DNS values, suggesting that the important effect of SGS unmixedness cannot be overlooked.

In Fig. 11(a) the variation of the streamwise averaged product across the shear layer evaluated from DNS, LES (with no model for the subgrid unmixedness) and FDF is shown. Consistent with the results shown in Fig. 10, it is observed that the FDF method reasonably well predicts the product distribution while the values calculated from LES method are significantly higher than the DNS values. The trend is similar at different Damkohler numbers. Furthermore it is shown in Fig. 11(b) that if the reaction source term is incorrectly calculated to be a function of the mean scalar values ($\overline{\omega}_\alpha = Da\overline{\phi}_A\overline{\phi}_B$) in the FDF approach, the corresponding results for $[\overline{\phi}_P]_x$ are similar to that evaluated from the LES method with

no reaction model. This is in accordance with the consistency of the Monte Carlo procedure and finite difference method as established above. The slight difference between the product profiles obtained from DNS and FDF methods in Fig. 11(a) is mainly due to inadequacy of the eddy viscosity type of closures to predict the velocity field. As a result, the transport of scalars (including the product) is not well captured by FDF (or LES) method. This issue is further discussed below where the possible remedies to resolve it is suggested.

The reasonably good prediction of the product formation by the FDF approach is due to capability of the method to explicitly calculate the nonlinear reaction source term. It is important that the reaction rate be correctly predicted by the model throughout the scalar evolution. In Fig. 12 the reaction source term calculated from the DNS, LES and FDF methods are shown at two different times. Consistent with the results in Fig. 11, the reaction rate term obtained from FDF method compares favorably with that of the DNS. The predicted reaction rate evaluated from LES method is much higher than the DNS values because the SGS unmixedness term is essentially ignored. The corresponding SGS unmixedness term is explicitly accounted for in the FDF method.

The robustness of the FDF method is further established in Fig. 13 where the sensitivity of the method to different parameters is tested. The results show that the product evaluated from the FDF method is essentially invariant to the number density of the particles provided that this density is not very low. Furthermore, it is observed that the chemical reaction is insensitive to the size of sample that is used to evaluate FDF. While the mean value of the scalar used in the mixing model for a given particle should be the mean value of the scalar at the particle location, it was observed that the mean value at the nearest finite difference grid point could be substituted. This eliminates the need for interpolating the mean scalar field to the particle locations. The result in both cases is essentially the same.

It was shown in Fig. 2(a) that the mean value of a conserved scalar ϕ calculated from FDF and LES methods are very close. As established mathematically, this similarity should always exist regardless of the values of mixing and flow parameters and also the type of models that are used for SGS stresses and scalar fluxes. This is confirmed in Fig. 14(a) where $[\overline{\phi}_A]_x$ for $Da = 0$ is shown. Additionally it is observed in this figure that at initial period of scalar evolution the LES and FDF values compare quite well with DNS values. However at latter times the difference between DNS and FDF (or LES) results is increased. The main reason

for this difference as explained before and as shown in Fig. 14 is the damping of the growth of shear layer that is caused by eddy diffusivity closures. Consistently, the reactant scalars also show a difference (although not very significant) between FDF and DNS results at later times of flow development (Fig. 14(b)). Expectedly, the deviation of the mean reactant values calculated from LES method with respect to DNS values is much more than that of the FDF.

The effectiveness of the FDF approach to predict the slightly more complex jet configuration is demonstrated in Fig. 15, where contours of the product mass fraction are plotted for the FDF, filtered DNS and LES (without reaction model). A resolution 151×76 is used in the FDF and LES simulations. A total of 20 particles per grid cell (yielding 80 particles per ensemble domain of $2\Delta x \times 2\Delta y$) were initialized at the start of the calculation. In order to reduce the computational expense, stochastic particles are only initialized in the region extending from $y = -1.75D$ to $y = 1.75D$ where y is the cross-stream coordinate and D is the jet diameter. New particles are introduced at the inlet only in this region at a rate proportional to the local flow velocity to maintain a constant particle density. It is assumed no reaction takes place in cells that do not contain particles. This approach requires that particles only be seeded in areas where the flow is undergoing chemical reaction yielding a considerable savings. The DNS is better represented in the FDF simulation than in the LES simulation, where the product formation in the coherent structures in considerably higher. This is further evidenced by Fig. 16 which shows the spatially evolving product thickness plotted as a function of the downstream coordinate. Additionally, Fig. 17 exhibits the time averaged product profiles as a function of the cross-stream coordinate at a downstream position of 2, 7 and 11 jet diameters. A critical assessment of these figures clearly indicates that neglect of the SGS unmixedness in the LES procedure results in gross errors in product formation while the FDF approach is able to resolve these effects and better predict the DNS data.

6 Conclusions

A filtered density function (FDF) method suitable for chemically reactive flows is developed in the context of large eddy simulation. The advantage of the FDF methodology is its inherent ability to resolve SGS scalar correlations that otherwise have to be modeled. Because of the lack of robust models to accurately predict these correlations in turbulent reactive flows, simulations involving turbulent combustion are often met with a degree of skepticism. The FDF methodology avoids the closure problem associated with these terms and treats the reaction in an exact manner. The scalar FDF approach is particularly attractive since it can be coupled with existing hydrodynamic CFD codes.

For conserved scalars the consistency between the FDF and moment closure approaches is demonstrated. This is observed by integrating the FDF transport equation to derive the corresponding moment equations. This consistency no longer exists in the reactive case and the benefits of the FDF approach are realized. No model is required in the FDF approach and thus the equivalent moment closure does not exist. The principle of equivalent systems is utilized in order to develop a tractable solution technique to indirectly calculate the FDF. A Lagrangian Monte Carlo method is employed to generate an equivalent system with the same FDF as that of true fluid particles.

Comparison of the FDF solution to that calculated by a conventional finite difference LES simulation utilizing a consistent moment closure yields favorable results for a conserved scalar. Such comparison is necessary to build confidence that the numerical particle method is capable to accurately capture the effects of convection, diffusion and mixing. Simulations of chemically reactive flows demonstrate the effectiveness of the FDF method in capturing the mean reaction rate. Comparison with a finite difference solution which does not attempt to model the SGS scalar covariance indicates the neglect of this term leads to unphysically high product conversion rates. Comparison of results between the FDF approach and those generated by DNS of two dimensional reacting shear layers and jets demonstrate that the FDF approach is capable of accurately capturing the primary features of unsteady combustion.

Although the present methodology has been developed for isothermal reactions, the extension

to exothermic variable density flows imposes no serious obstacles and is currently under investigation by the authors. With the generalization to reactive flows with heat release, arbitrarily complicated reaction schemes may be implemented with little difficulty since no special treatment is necessary for the source terms in the FDF approach. The scalar domain must be modified to include the temperature (or energy) so that any correlations involving temperature may be evaluated. Utilizing such a scalar FDF approach, it is conceivable that LES of complex reactive flows with realistic chemical kinetics may be routinely simulated for engineering applications in the near future. The fact that the scalar FDF approach avoids the closure problem for the source terms is significant as no model has yet been proposed for use in LES which has universal applicability. This is the primary stumbling block for implementation of LES to evaluate unsteady combustion processes. Even for the simple chemistry scheme considered in this study there are many difficulties in evaluating the nonlinear reaction source term by conventional LES methods. This term is closed in the FDF approach and imposes no difficulty even if the reaction takes on a more complex form.

One drawback of the scalar FDF approach is that any correlations involving the velocity field (such as SGS stresses and SGS mass and heat fluxes) must be modeled using existing gradient diffusion models. This drawback may be readily overcome by considering the joint velocity-scalar FDF in which the velocity correlations appear in closed form eliminating the dependence on such models (Pope, 1985). This area has seen considerable development in the area of RANS (Pope, 1994). Improvement in the prediction of the subgrid viscosity is also necessary (and perhaps more significant) in the estimation of the turbulent frequency in the molecular mixing model. The extension of FDF method to include the velocity domain is also the subject of current investigation.

7 Personnel

The Co-PIs of this project are Drs. Peyman Givi, Cyrus K. Madnia and Dale B. Taulbee. Two Graduate Research Assistants (RAs) have been supported directly by this Grant: (1) Mr. Paul Colucci and (2) Mr. Virgil Adumitroaie. Mr. Colucci is involved in task (1) and Mr. Adumitroaie is responsible for task (2).

Considering the diversity of this research we have had to involve several additional students. The following are also contributing to this project but are not financially supported by NASA: Dr. Farhad Jaberi, Mr. Laurent Gicquel and Mr. Sean Garrick. Dr. Jaberi is assisting Mr. Colucci in task (1), Mr. Gicquel is solely responsible for task (3) and Mr. Garrick is responsible for task (4).

Acknowledgment:

We are indebted to Professor Stephen B. Pope for many technical discussions and very useful comments through the course of this research.

References

Aldama, A. A. (1990). *Filtering Techniques for Turbulent Flow Simulations*, volume 49 of *Lecture Notes in Engineering*. Springer-Verlag, New York, NY.

Bardina, J., Ferziger, J. H., and Reynolds, W. C. (1983). Improved turbulence models based on large eddy simulations of homogeneous, incompressible, turbulent flows. Department of Mechanical Engineering Report TF-19, Stanford University, Stanford, CA.

Billingsly, P. (1979). *Probability and Measure*. John Wiley and Sons, Inc., New York.

Bockhorn, H. (1988). Finite chemical reaction rate and local equilibrium effects in turbulent hydrogen-air diffusion flames. In *Proceedings of the 22nd Symp. (Int.) on Combustion*, pages 665–664. The Combustion Institute, Pittsburgh, PA.

Brodkey, R. S., editor. (1975). *Turbulence in Mixing Operation*. Academic Press, New York, NY.

Brodkey, R. S. (1981). Fundamental of turbulent motion. *Chem. Eng. Comm.* **8**, 1–23.

Carpenter, M. H. (1990). A high-order compact numerical algorithm for supersonic flows. In Morton, K. W., editor, *Twelfth International Conference on Numerical Methods in Fluid Dynamics*, volume 371 of *Lecture Notes in Physics*, pages 254–258. Springer-Verlag, New York, NY.

Chorin, A. J. and Marsden, J. E. (1979). *A Mathematical Introduction to Fluid Mechanics*. Springer-Verlag, New York, NY.

Chorin, A. J. (1968). Numerical solution of the Navier-Stokes equations. *Math. Comp.* **22**, 745–763.

Cook, A. W. and Riley, J. J. (1994). A subgrid model for equilibrium chemistry in turbulent flows. *Phys. Fluids* **6**, 2868–2870.

Curl, R. L. (1963). Dispersed phase mixing: I. Theory and effects in simple reactors. *AIChE J.* **9**, 175–181.

Dopazo, C. and O'Brien, E. E. (1976). Statistical treatment of non-isothermal chemical reactions in turbulence. *Combust. Sci. and Tech.* **13**, 99–112.

Dopazo, C. (1994). Recent developments in pdf methods. In Libby and Williams (1994), chapter 7, pages 375–474.

Frankel, S. H., Adumitroaie, V., Madnia, C. K., and Givi, P. (1993). Large eddy simulations of turbulent reacting flows by assumed PDF methods. In Ragab, S. A. and Piomelli, U., editors, *Engineering Applications of Large Eddy Simulations*, pages 81–101. ASME, FED-Vol. 162, New York, NY.

Frankel, S. H., Madnia, C. K., and Givi, P. (1993). Comparative assessment of closures for turbulent reacting flows. *AIChE J.* **39**, 899–903.

Frankel, S. H. (1993), *Probabilistic and Deterministic Description of Turbulent Flows with Nonpremixed Reactants.* Ph.D. Thesis, Department of Mechanical and Aerospace Engineering, State University of New York at Buffalo, Buffalo, NY.

Fureby, C. and Lofstrom, C. (1994). Large-eddy simulations of bluff body stabilized flames. In *Proceedings of 25th Symp. (Int.) on Combustion*, pages 1257–1264. The Combustion Institute, Pittsburgh, PA.

Galperin, B. and Orszag, S. A., editors. (1993). *Large Eddy Simulations of Complex Engineering and Geophysical Flows.* Cambridge University Press, Cambridge, UK.

Gao, F. and O'Brien, E. E. (1993). A large-eddy simulation scheme for turbulent reacting flows. *Phys. Fluids A* **5**, 1282–1284.

Gardiner, C. W. (1990). *Handbook of Stochastic Methods.* Springer-Verlag, New York, NY.

Garrick, S. C. (1995). Large eddy simulations of a turbulent reacting mixing layer. AIAA Paper 95-0010.

Germano, M., Piomelli, U., Moin, P., and Cabot, W. H. (1991). A dynamic subgrid-scale eddy viscosity model. *Phys. Fluids A* **3**, 1760–1765.

Germano, M. (1986). A proposal for a redefinition of the turbulent stresses in the filtered navier-stokes equations. *Phys. Fluids* **29**, 2323–2324.

Germano, M. (1992). Turbulence: The filtering appraoch. *J. Fluid Mech.* **238**, 325–336.

Ghoniem, A. F. (1991). Vortex simulation of reacting shear flow. In Oran and Boris (1991), chapter 10, pages 305–348.

Gillespie, D. T. (1992). *Markov Processes, An Introduction for Physical Scientists.* Academic Press, New York, NY.

Givi, P. (1989). Model free simulations of turbulent reactive flows. *Prog. Energy Combust. Sci.* **15**, 1–107.

Givi, P. (1994). Spectral and random vortex methods in turbulent reacting flows. In Libby and Williams (1994), chapter 8, pages 475–572.

Gustafson, K. E. and Sethian, J. A., editors. (1991). *Vortex Methods and Vortex Motion.* SIAM, Philadelphia, PA.

Helfand, E. (1979). Numerical integration of stochastic differential equations. *Bell System Technical Journal* **58**, 2289 – 2299.

Hill, J. C. (1976). Homogeneous turbulent mixing with chemical reaction. *Ann. Rev. Fluid Mech.* **8**, 135–161.

Janicka, J. and Kollmann, W. (1979). A two-variables formalism for the treatment of chemical reactions in turbulent H_2-air diffusion flames. In *Proceedings of 17th Symp. (Int.) on Combustion*, pages 421–430. The Combustion Institute, Pittsburgh, PA.

Janicka, J., Kolbe, W., and Kollmann, W. (1979). Closure of the transport equation for the probability density function of turbulent scalar field. *J. Nonequil. Thermodyn.* **4**, 47–66.

Jones, W. P. and Priddin, C. H. (1978). Predictions of the flowfield and local gas composition in gas turbine combustors. In *17th Symp. (Int.) on Combustion*, pages 399–409. The Combustion Institute, Pittsburgh, PA.

Jones, W. P. and Whitelaw, J. H. (1984). Modelling and measurements in turbulent combustion. In *20th Symp. (Int.) on Combustion*, pages 233–249. The Combustion Institute, Pittsburgh, PA.

Jones, W. P. (1994). Turbulence modelling and numerical solution methods for variable density and combusting flows. In Libby and Williams (1994), chapter 6, pages 309–374.

Karlin, S. and Taylor, H. M. (1981). *A Second Course in Stochastic Processes.* Academic Press, New York, NY.

Kerr, R. M., Domaradzki, J. A., and Barbier, G. (1996). Small-scale properties of nonlinear interactions and subgrid-scale energy transfer in isotropic turbulence. *Phys. Fluids* **8**, 197–208.

Kloeden, P. E. and Platen, E. (1995). *Numerical Solution of Stochastic Differential Equations*, volume 23 of *Applications of Mathematics, Stochastic Modelling and Applied Probability.* Springer-Verlag, New York, NY.

Kosály, G. and Givi, P. (1987). Modeling of turbulent molecular mixing. *Combust. Flame* **70**, 101–118.

Leonard, A. (1974). Energy cascade in large-eddy simulations of turbulent flows. *Advances in Geophys.* **18A**, 237–248.

Leonard, A. (1980). Vortex methods for flow simulation. *J. Comp. Phys.* **37**, 289–335.

Libby, P. A. and Williams, F. A., editors. (1980). *Turbulent Reacting Flows*, volume 44 of *Topics in Applied Physics*. Springer-Verlag, Heidelberg.

Libby, P. A. and Williams, F. A., editors. (1994). *Turbulent Reacting Flows*. Academic Press, London, UK.

Lilly, D. K. (1965). On the computational stability of numerical solutions of time-dependent non-linear geophysical fluid dynamics problems. *Monthly Weather Review* **93**, 11–26.

Lilly, D. K. (1967). The representation of small-scale turbulence in numerical simulation experiments. In *Proceedings of IBM Scientific Computing Symposium Environmental Sciences*, pages 195–210. IBM Form No. 320-1951.

Lilly, D. K. (1992). A proposed modification of the Germano subgrid-scale closure method. *Phys. Fluids A* **4**, 633–634.

Liou, T. M., Lien, W. Y., and Hwang, P. W. (1994). Large-eddy simulations of turbulent reacting flows in chamber with gaseous ethylene injecting through the porous wall. *Combust. Flame* **99**, 591–600.

Lockwood, F. C. and Moneib, H. A. (1980). Fluctuating temperature measurement in a heated round free jet. *Combust. Sci. and Tech.* **22**, 63–81.

Lumley, J. L., editor. (1990). *Whither Turbulence? Turbulence at the Crossroads*, volume 357 of *Lecture Notes in Physics*. Springer-Verlag, New York, NY.

Lundgren, T. S. (1967). Distribution functions in the statistical theory of turbulence. *Phys. Fluids* **10**, 969–975.

Lundgren, T. S. (1972). In Rosenblatt, H. and Atta, C. Ven, editors, *Statistical Models and Turbulence*, page 70. Springer-Verlag, New York, NY.

Madnia, C. K. and Givi, P. (1993). Direct numerical simulation and large edddy simulation of reacting homogeneous turbulence. In Galperin and Orszag (1993), chapter 15, pages 315–346.

Madnia, C. K., Frankel, S. H., and Givi, P. (1992). Reactant conversion in homogeneous turbulence: Mathematical modeling, computational validations and practical applications. *Theoret. Comput. Fluid Dynamics* **4**, 79–93.

Majda, A. (1988). Vortex dynamics: Numerical analysis, scientific computing, and mathematical theory. In McKenna, J. and Temam, R., editors, *ICIAM '87*, pages 153–182. Society for Industrial and Applied Mathematics, Philadelphia.

McMurtry, P. A. and Givi, P. (1989). Direct numerical simulations of mixing and reaction in a nonpremixed homogeneous turbulent flow. *Combust. Flame* **77**, 171–185.

Miller, R. S., Frankel, S. H., Madnia, C. K., and Givi, P. (1993). Johnson-Edgeworth translation for probability modeling of binary scalar mixing in turbulent flows. *Combust. Sci. and Tech.* **91**, 21–52.

Moin, P., Squires, W., Cabot, W. H., and Lee, S. (1991). A dynamic subgrid-scale model for compressible turbulence and scalar transport. *Phys. Fluids A* **3**, 2746–2757.

O'Brien, E. E. (1980). The probability density function (PDF) approach to reacting turbulent flows. In Libby and Williams (1980), chapter 5, pages 185–218.

Oran, E. S. and Boris, J. P., editors. (1991). *Numerical Approaches to Combustion Modeling*, volume 135 of *Progress in Astronautics and Aeronautics*. AIAA Publishing Co., New York, NY.

Papoulis, A. (1965). *Probability, Random Variables, and Stochastic Processes*. McGraw-Hill Book Company, New York, NY.

Pope, S. B. (1976). The probability approach to modeling of turbulent reacting flows. *Combust. Flame* **27**, 299–312.

Pope, S. B. (1979). The statistical theory of turbulent flames. *Phil. Trans. Royal Soc. London* **291**, 529–568.

Pope, S. B. (1981). A Monte Carlo method for the PDF equations of turbulent reactive flow. *Combust. Sci. and Tech.* **25**, 159–174.

Pope, S. B. (1982). An improved turbulent mixing model. *Combust. Sci. and Tech.* **28**, 131–145.

Pope, S. B. (1985). PDF methods for turbulent reactive flows. *Prog. Energy Combust. Sci.* **11**, 119–192.

Pope, S. B. (1990). Computations of turbulent combustion: Progress and challenges. In *Proceedings of 23rd Symp. (Int.) on Combustion*, pages 591–612. The Combustion Institute, Pittsburgh, PA.

Pope, S. B. (1994). Lagrangian pdf methods for turbulent flows. *Ann. Rev. Fluid Mech.* **26**, 23–63.

Priddin, C. H. (1991). Turbulent combustion modeling-A review. In Johansson, A. V. and Alfredsson, P. H., editors, *Advances in Turbulence 3*, pages 279–299. Springer-Verlag, Berlin.

Reynolds, W. C. (1990). The potential and limitations of direct and large eddy simulations. In Lumley (1990), pages 313–343.

Rhodes, P. R. (1975). A probability distribution function for turbulent flows. In Murthy, S. N. B., editor, *Turbulent Mixing in Non-Reactive and Reactive Mixing*, pages 235–241. Plenum Press, New York, NY.

Risken, H. (1989). *The Fokker-Planck Equation, Methods of Solution and Applications.* Springer-Verlag, New York, NY.

Rogallo, R. S. and Moin, P. (1984). Numerical simulation of turbulent flow. *Ann. Rev. Fluid Mech.* **16**, 99–137.

Ross, S. (1996). *Stochastic Processes.* John Wiley and Sons, New York, NY.

Sarpkaya, T. (1989). Computational methods with vortices - the 1988 freeman scholar lecture. *Journal of Fluids Engineering* **111**, 5–52.

Schumann, U. (1989). Large eddy simulation of turbulent diffusion with chemical reactions in the convective boundary layer. *Atmospheric Environment* **23**, 1713–1726.

Schuss, Z. (1980). *Theory and Applications of Stochastic Eifferential Equations.* John Wiley and Sons, Inc., New York.

Smagorinsky, J. (1963). General circulation experiments with the primitive equations. I. The basic experiment. *Monthly Weather Review* **91**, 99–164.

Spalding, D. B. (1977). Development of the eddy-break-up model of turbulent combustion. In *Proceedings of 16th Symp. (Int.) on Combustion*, page 1657. The Combustion Institute, Pittsburgh, PA.

Stratonovich, R. L. (1963). *Introduction to the Theory of Random Noise.* Gordon and Breach, New York, NY.

Toor, H. L. (1962). Mass transfer in dilute turbulent and nonturbulent systems with rapid irreversible reactions and equal diffusivities. *AIChE J.* **8**, 70–78.

Toor, H. L. (1975). The non-premixed reaction: $A + B \rightarrow$ *Products*. In Brodkey (1975), pages 123–166.

Voke, P. R. and Collins, M. W. (1983). Large eddy simulation: Retrospect and prospects. *PhysicoChemical Hydrodynamics* **4**, 119–161.

Zang, T. A., Krist, S. E., and Hussaini, M. Y. (1989). Resolution requirements for numerical simulations of transition. *J. Sci. Comput.* **14**, 197–217.

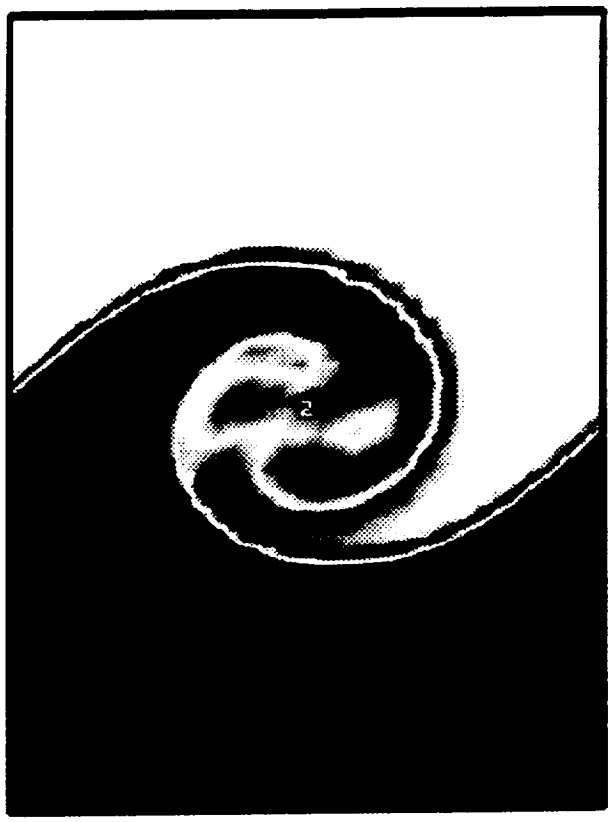

(a)

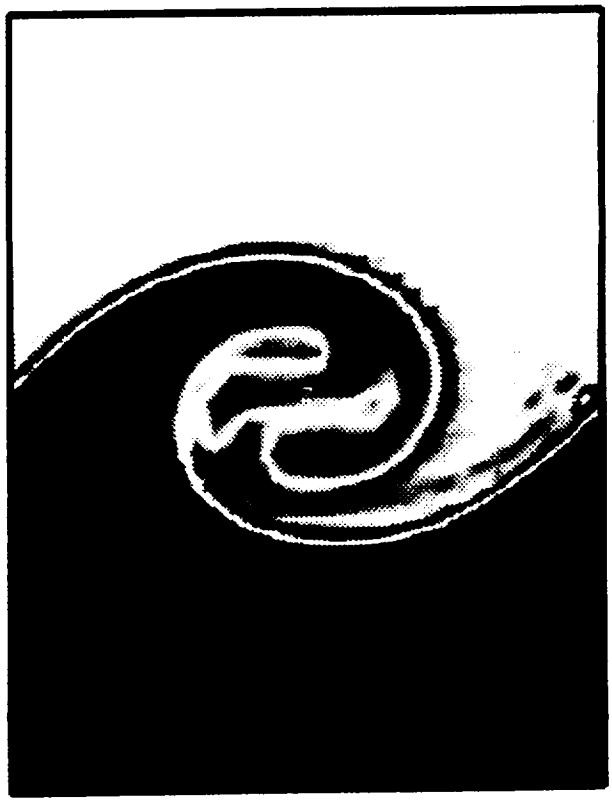

Figure 1

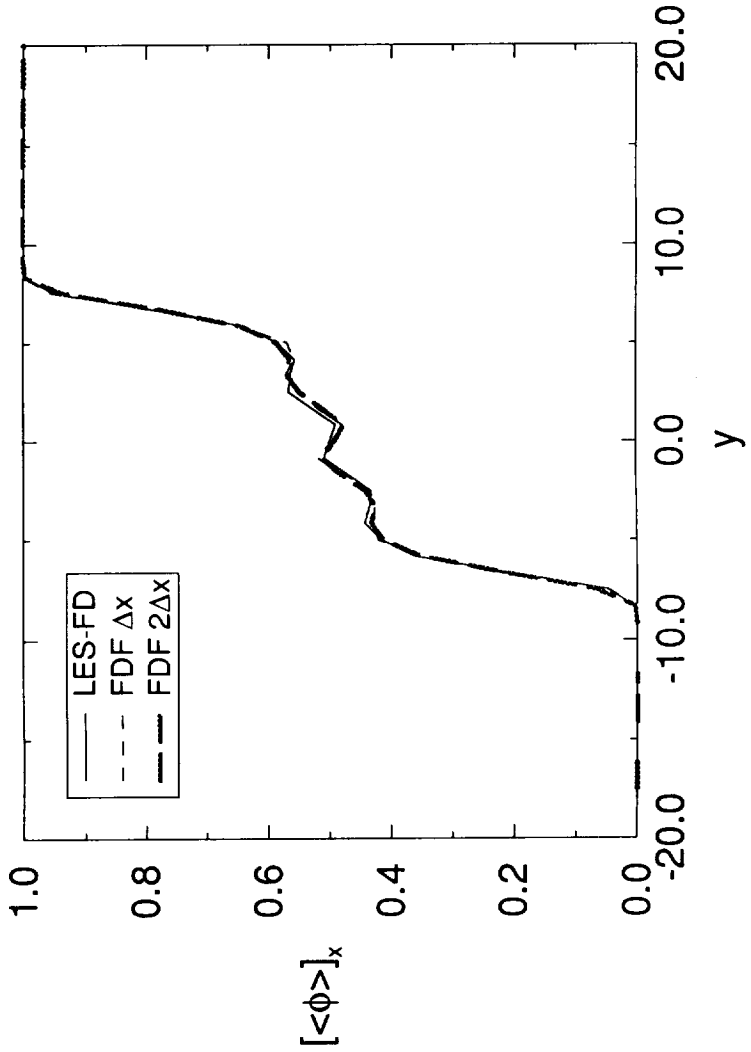

Figure 2 (a)

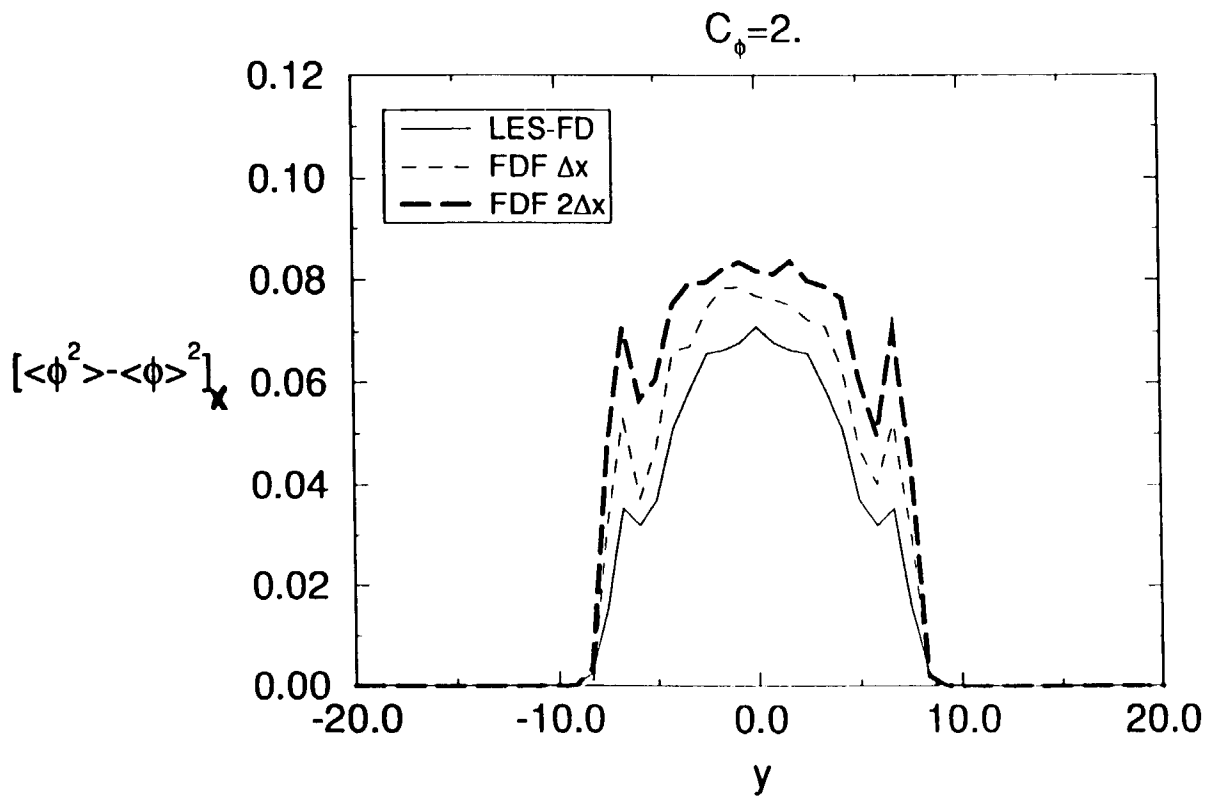
C_ϕ=2.
LES-FD
FDF Δx
FDF 2Δx
$[<\phi^2>-<\phi>^2]_x$
0.12
0.10
0.08
0.06
0.04
0.02
0.00
-20.0
-10.0
0.0
10.0
20.0
y

Figure 2 (b)

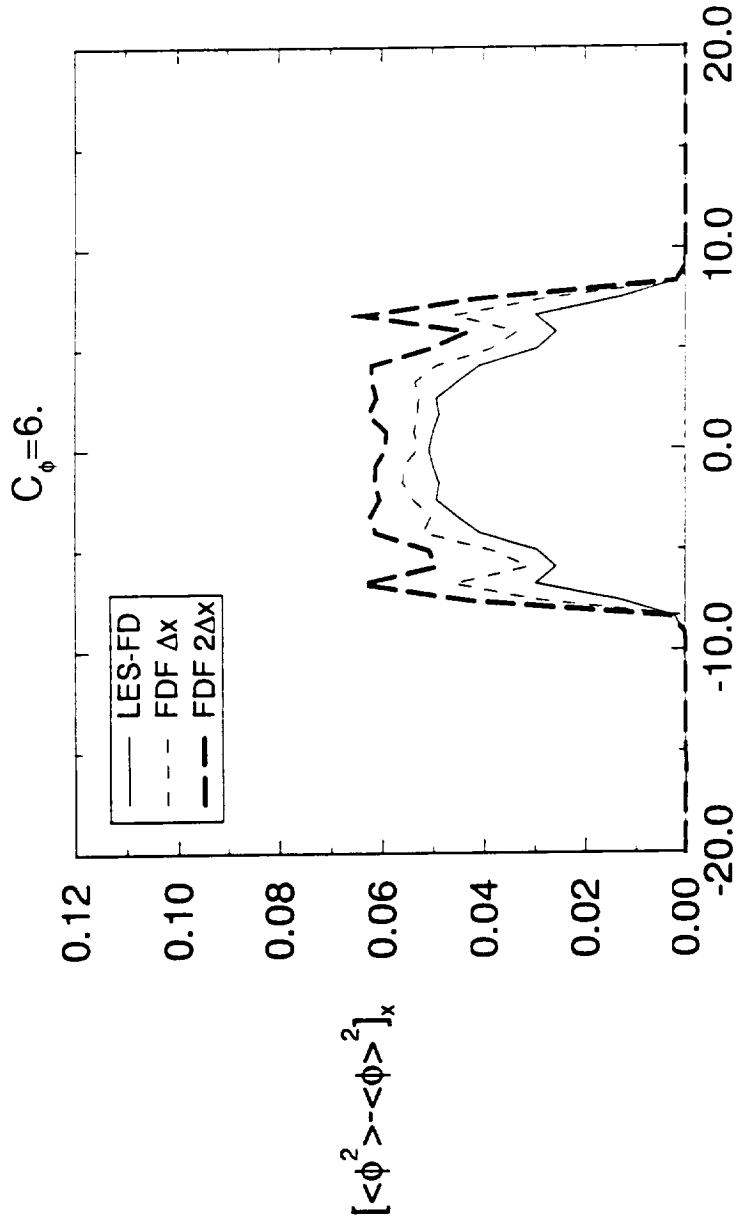
C_ϕ=6.
LES-FD
FDF Δx
FDF 2Δx
0.12
0.10
0.08
0.06
0.04
0.02
0.00
$[<\phi^2>-<\phi>^2]_x$
-20.0
-10.0
0.0
10.0
20.0
y

Figure 2(c)

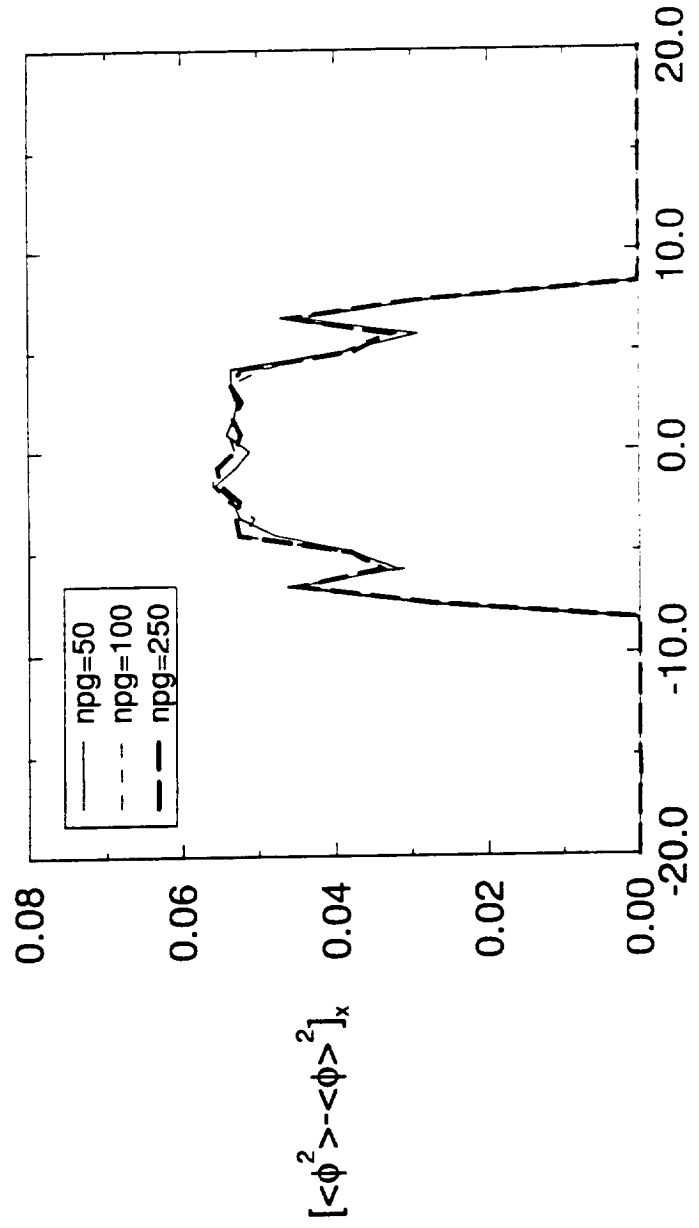
npg=50
npg=100
npg=250
0.08
0.06
0.04
0.02
0.00
-20.0
-10.0
0.0
10.0
20.0
y
$[<\phi^2>-<\phi>^2]_x$

Figure 3(a)

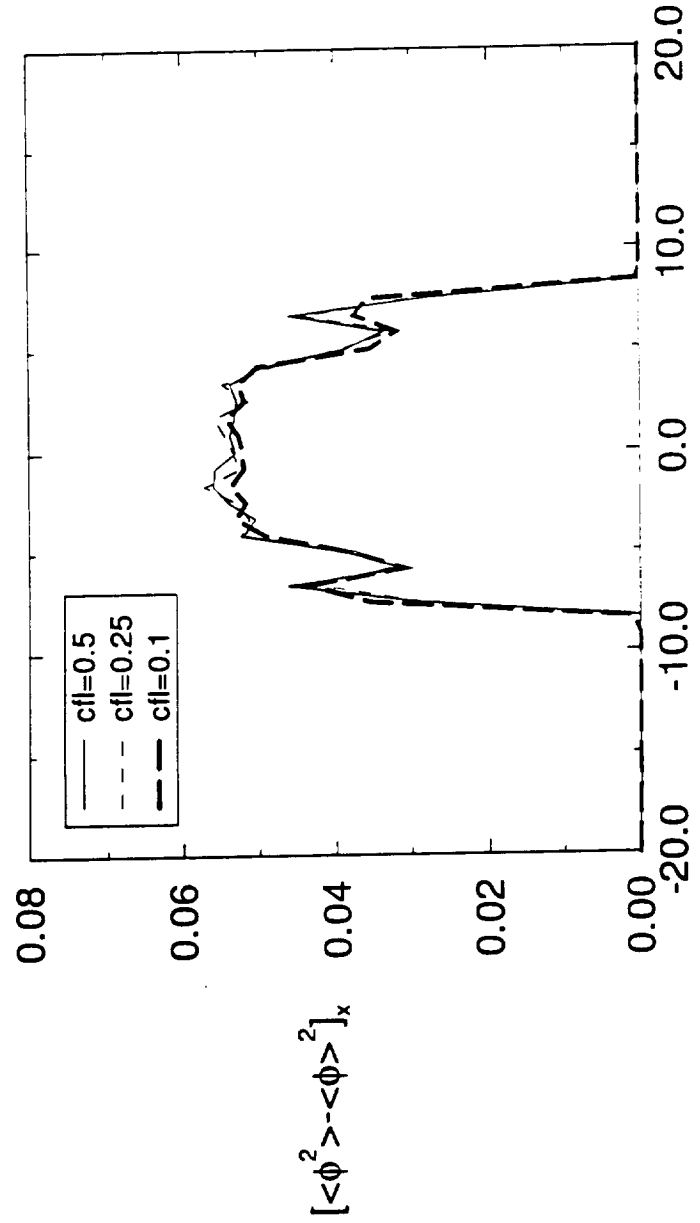
cfl=0.5
cfl=0.25
cfl=0.1
0.08
0.06
0.04
0.02
0.00
-20.0
-10.0
0.0
10.0
20.0
y
$[<\phi^2>-<\phi>^2]_x$

Figure 3 (b)

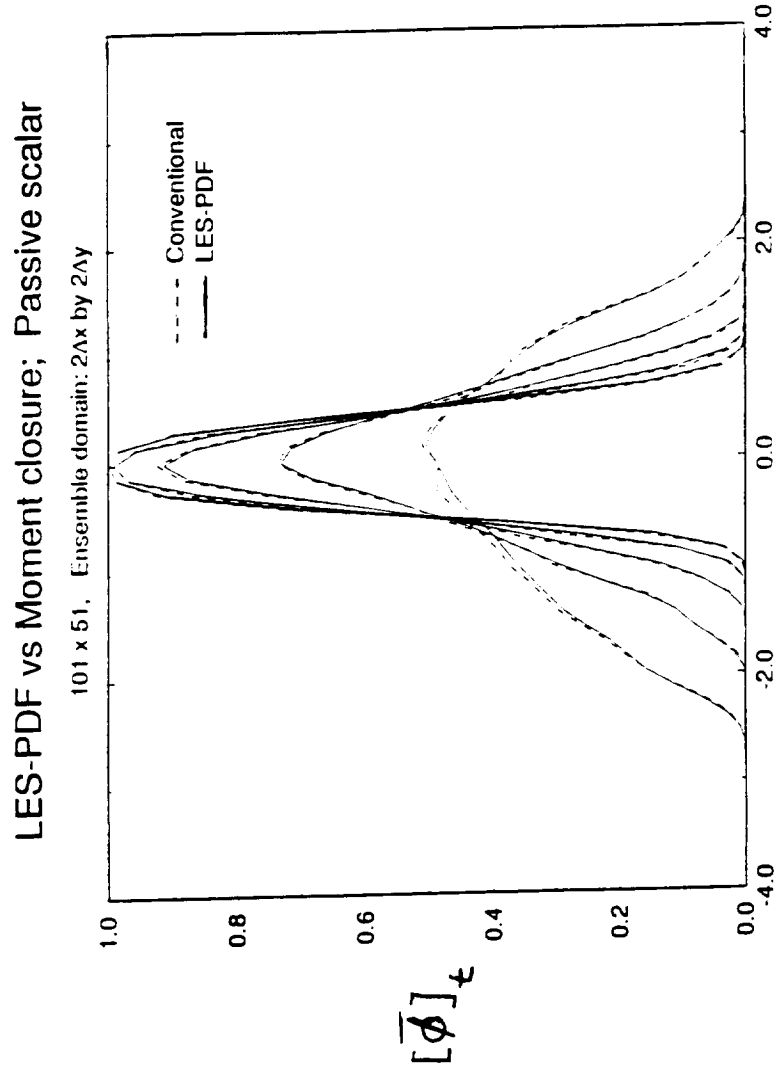
LES-PDF vs Moment closure; Passive scalar
101 x 51, Ensemble domain: 2Δx by 2Δy
Conventional
LES-PDF
$[\overline{\phi}]_t$
y
1.0
0.8
0.6
0.4
0.2
0.0
-4.0
-2.0
0.0
2.0
4.0

Figure 4

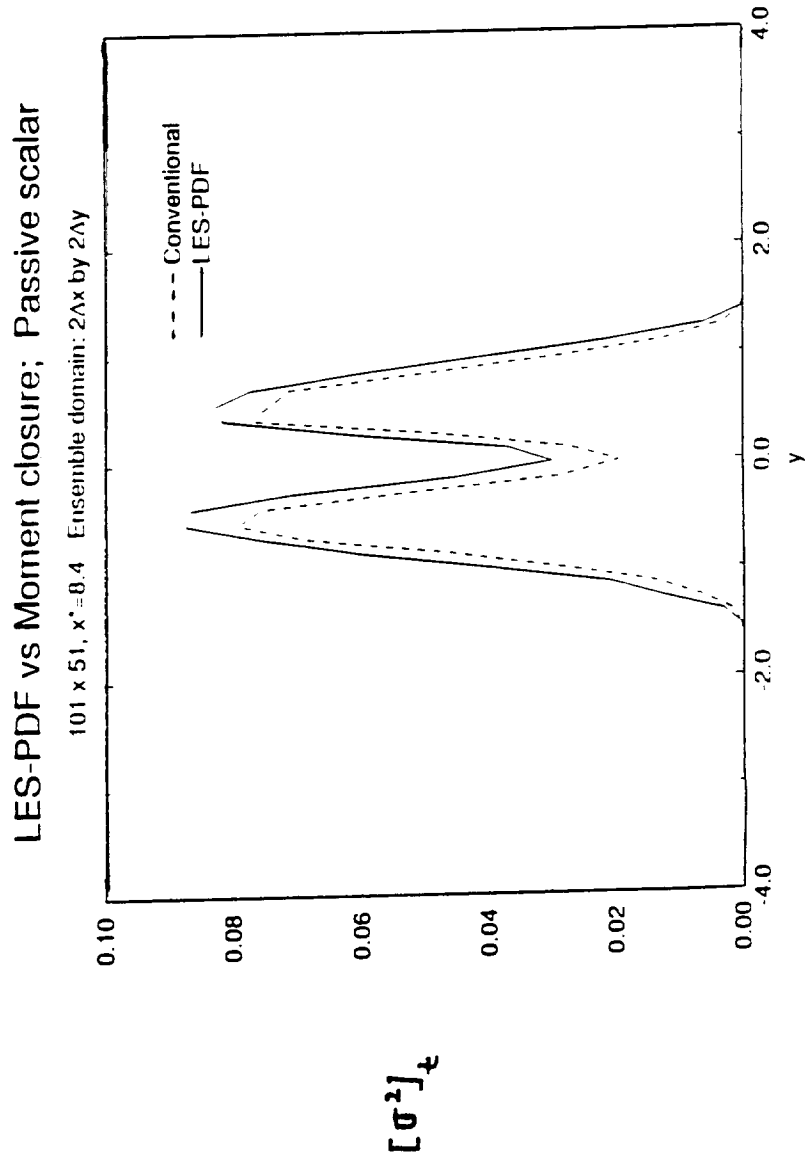
LES-PDF vs Moment closure; Passive scalar
101 x 51, x*=8.4 Ensemble domain: 2Δx by 2Δy
Conventional
LES-PDF
0.10
0.08
0.06
0.04
0.02
0.00
-4.0
-2.0
0.0
2.0
4.0
y
$[\sigma^2]_t$

Figure 5 (a)

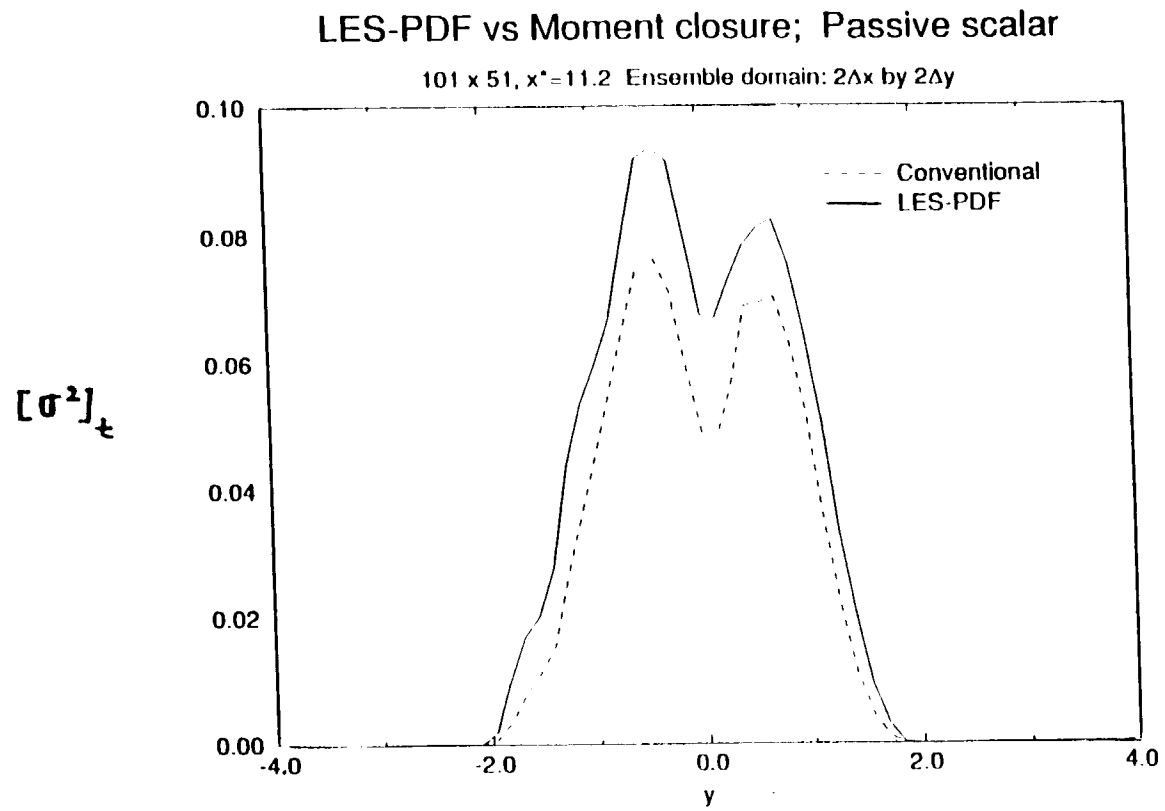
LES-PDF vs Moment closure; Passive scalar
101 x 51, x*=11.2 Ensemble domain: 2Δx by 2Δy
$[\sigma^2]_t$
0.10
0.08
0.06
0.04
0.02
0.00
-4.0
-2.0
0.0
2.0
4.0
y
Conventional
LES-PDF

Figure 5 (b)

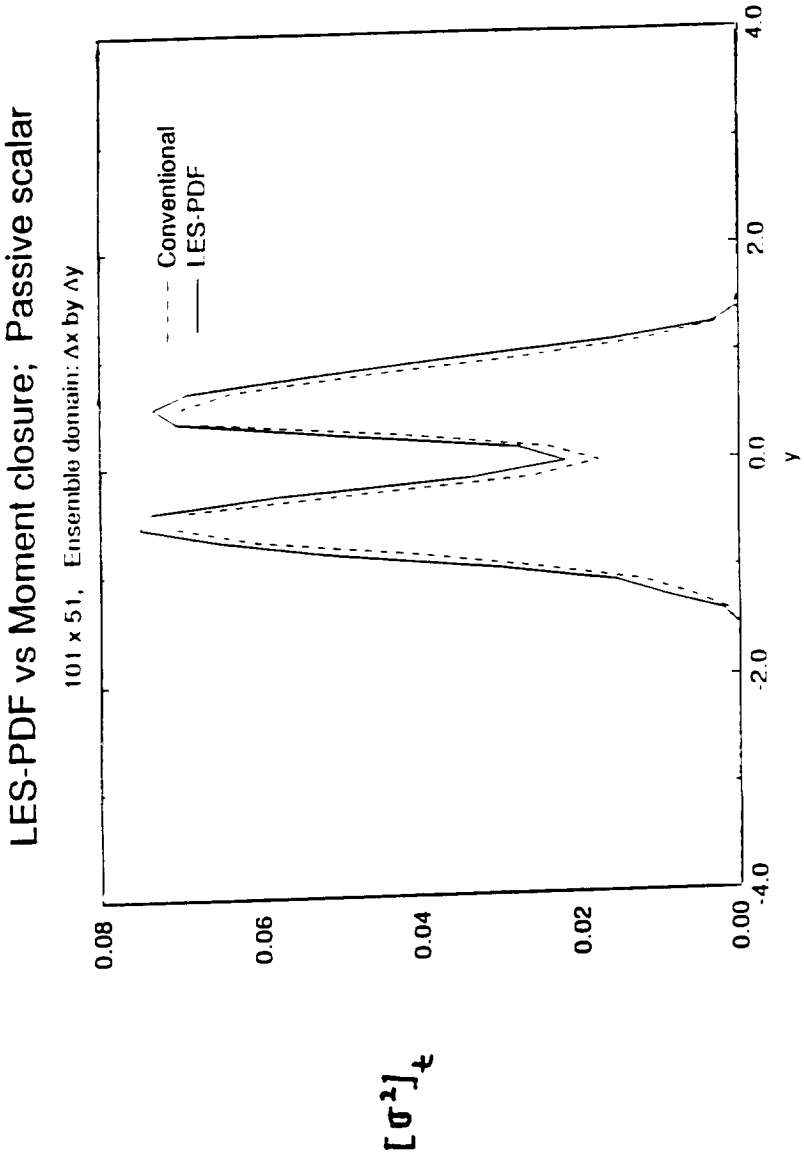
LES-PDF vs Moment closure; Passive scalar
101 x 51, Ensemble domain: Δx by Δy
Conventional
LES-PDF
0.08
0.06
0.04
0.02
0.00
-4.0
-2.0
0.0
2.0
4.0
y
$[\sigma^2]_t$

Figure 5(c)

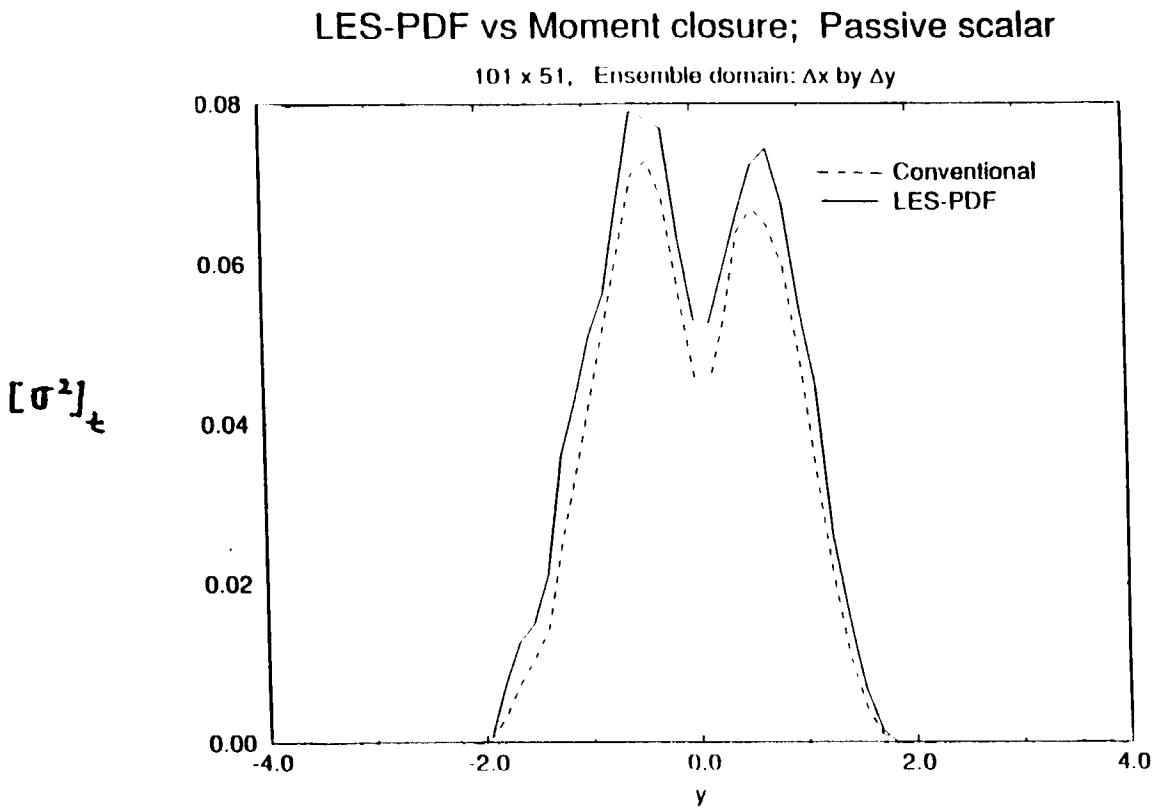

$[\sigma^2]_t$

Figure 5(d)

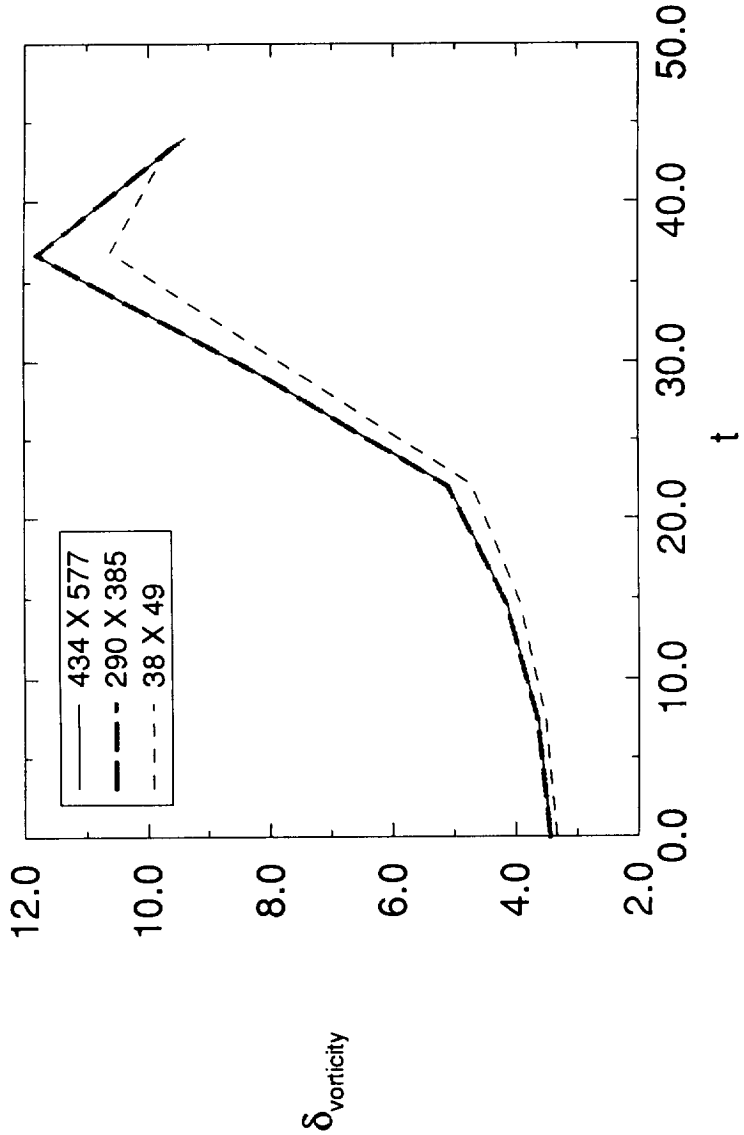
12.0
10.0
8.0
6.0
4.0
2.0
0.0
10.0
20.0
30.0
40.0
50.0
t
$\delta_{vorticity}$
434 X 577
290 X 385
38 X 49

Figure 6 (a)

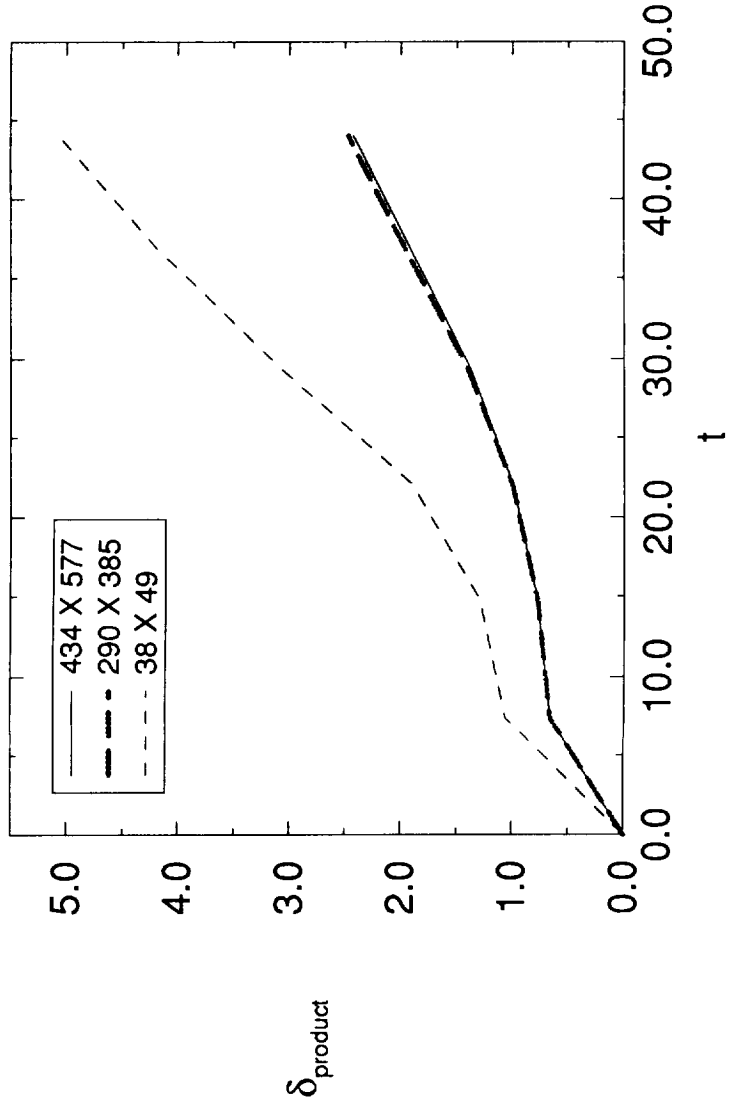
434 X 577
290 X 385
38 X 49
5.0
4.0
3.0
2.0
1.0
0.0
0.0
10.0
20.0
30.0
40.0
50.0
t
$\delta_{product}$

Figure 6 (b)

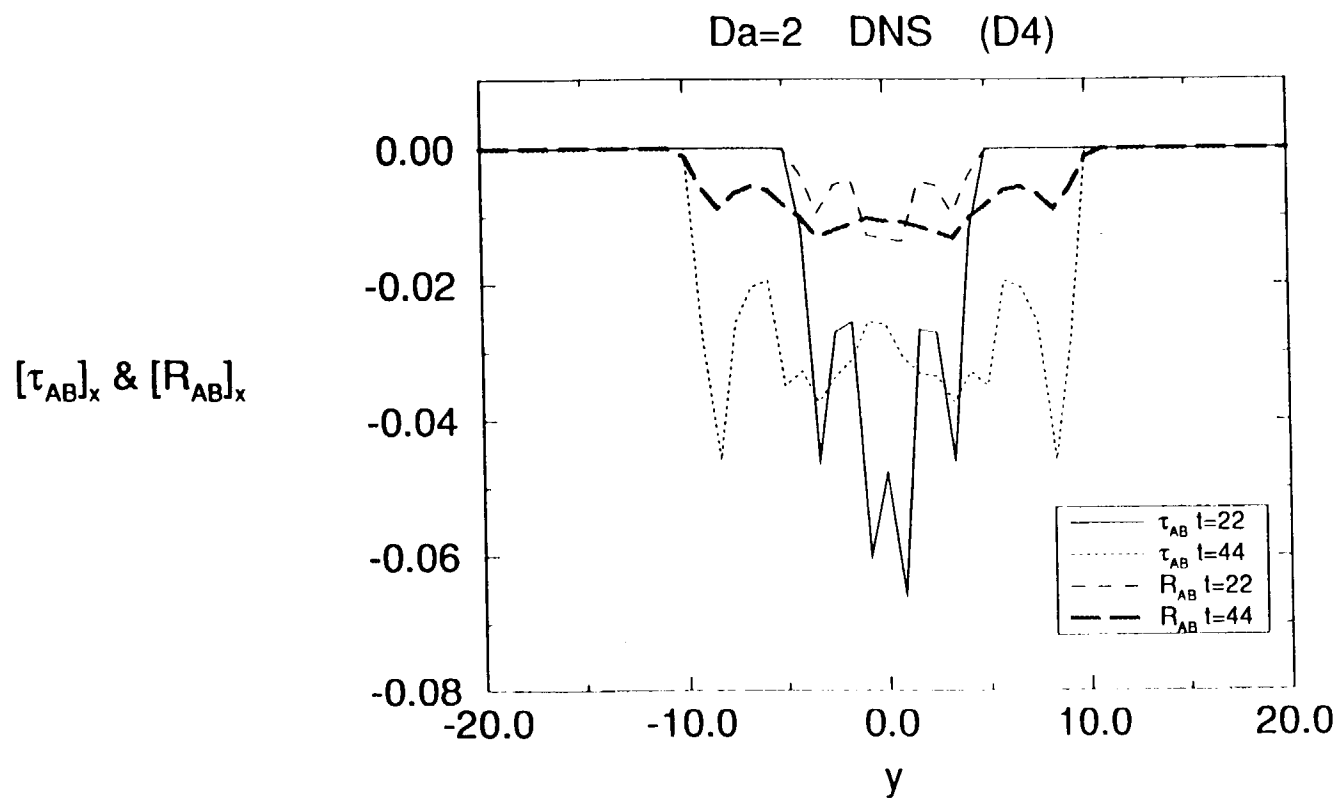
Da=2 DNS (D4)
$[\tau_{AB}]_x$ & $[R_{AB}]_x$
0.00
-0.02
-0.04
-0.06
-0.08
-20.0
-10.0
0.0
10.0
20.0
y
τ_{AB} t=22
τ_{AB} t=44
R_{AB} t=22
R_{AB} t=44

Figure 7

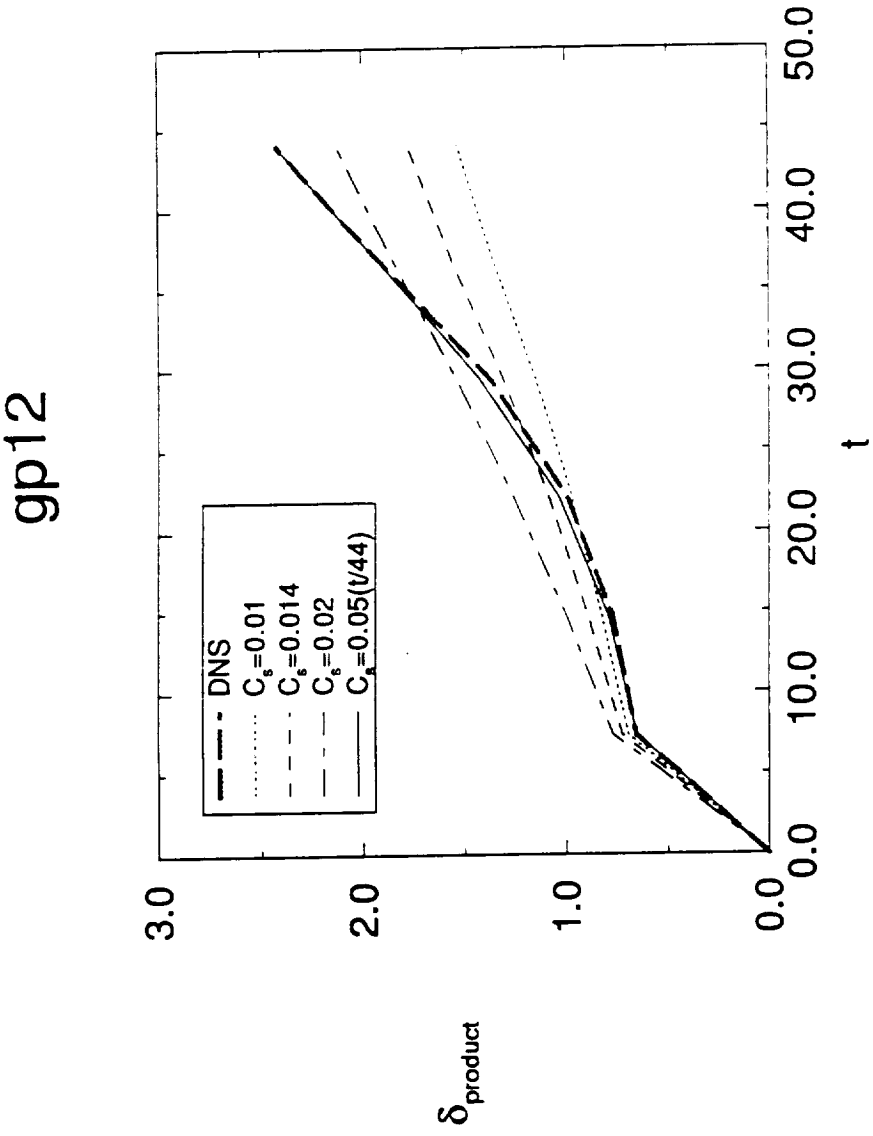
gp12
DNS
C_s=0.01
C_s=0.014
C_s=0.02
C_s=0.05(t/44)
$\delta_{product}$
t
0.0
1.0
2.0
3.0
0.0
10.0
20.0
30.0
40.0
50.0

Figure 8

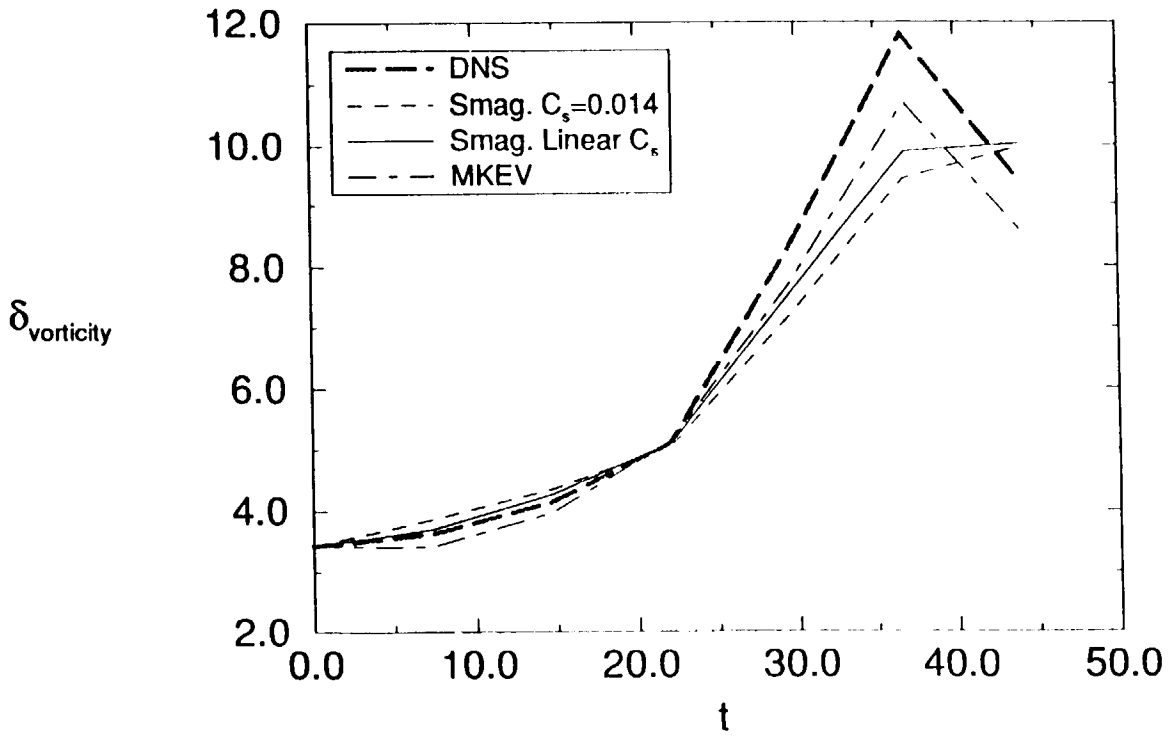
12.0
10.0
8.0
6.0
4.0
2.0
0.0
10.0
20.0
30.0
40.0
50.0
t
$\delta_{vorticity}$
DNS
Smag. C_s=0.014
Smag. Linear C_s
MKEV

Figure 9

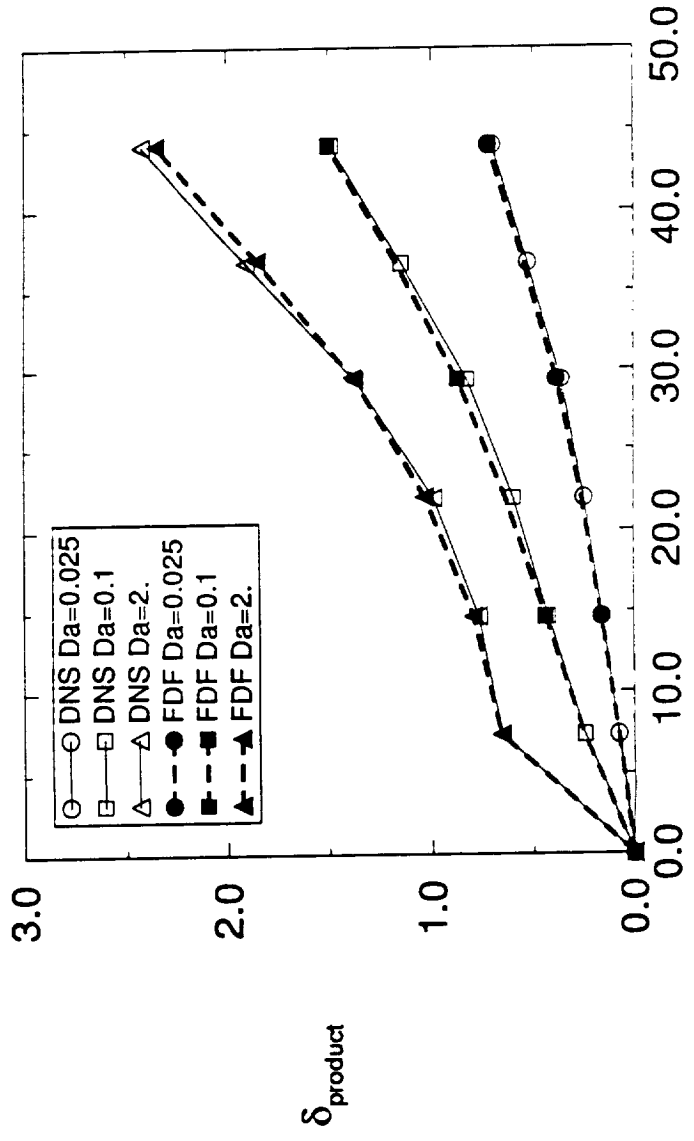
gp13
DNS Da=0.025
DNS Da=0.1
DNS Da=2.
FDF Da=0.025
FDF Da=0.1
FDF Da=2.
3.0
2.0
1.0
0.0
0.0
10.0
20.0
30.0
40.0
50.0
t
$\delta_{product}$

Figure 10(a)

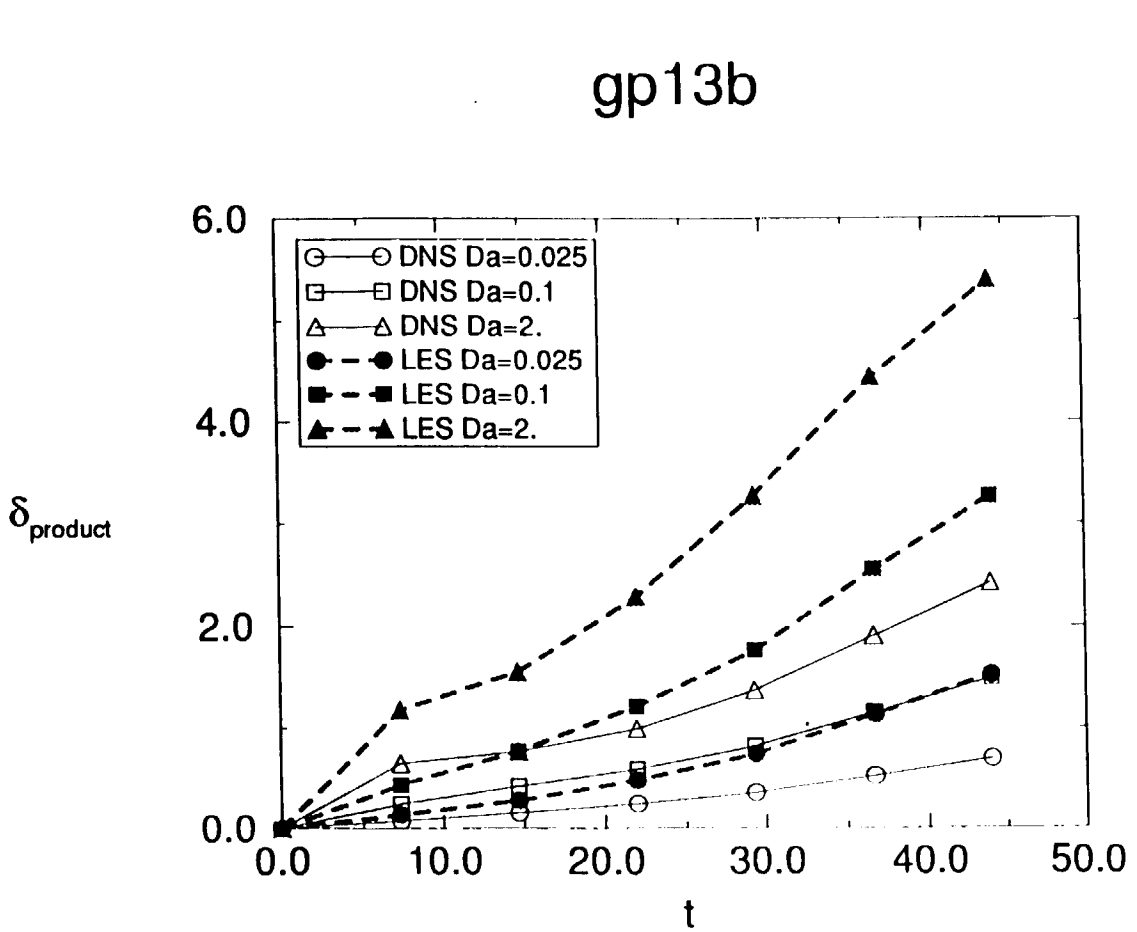
gp13b
DNS Da=0.025
DNS Da=0.1
DNS Da=2.
LES Da=0.025
LES Da=0.1
LES Da=2.
$\delta_{product}$
6.0
4.0
2.0
0.0
0.0
10.0
20.0
30.0
40.0
50.0
t

Figure 10 (b)

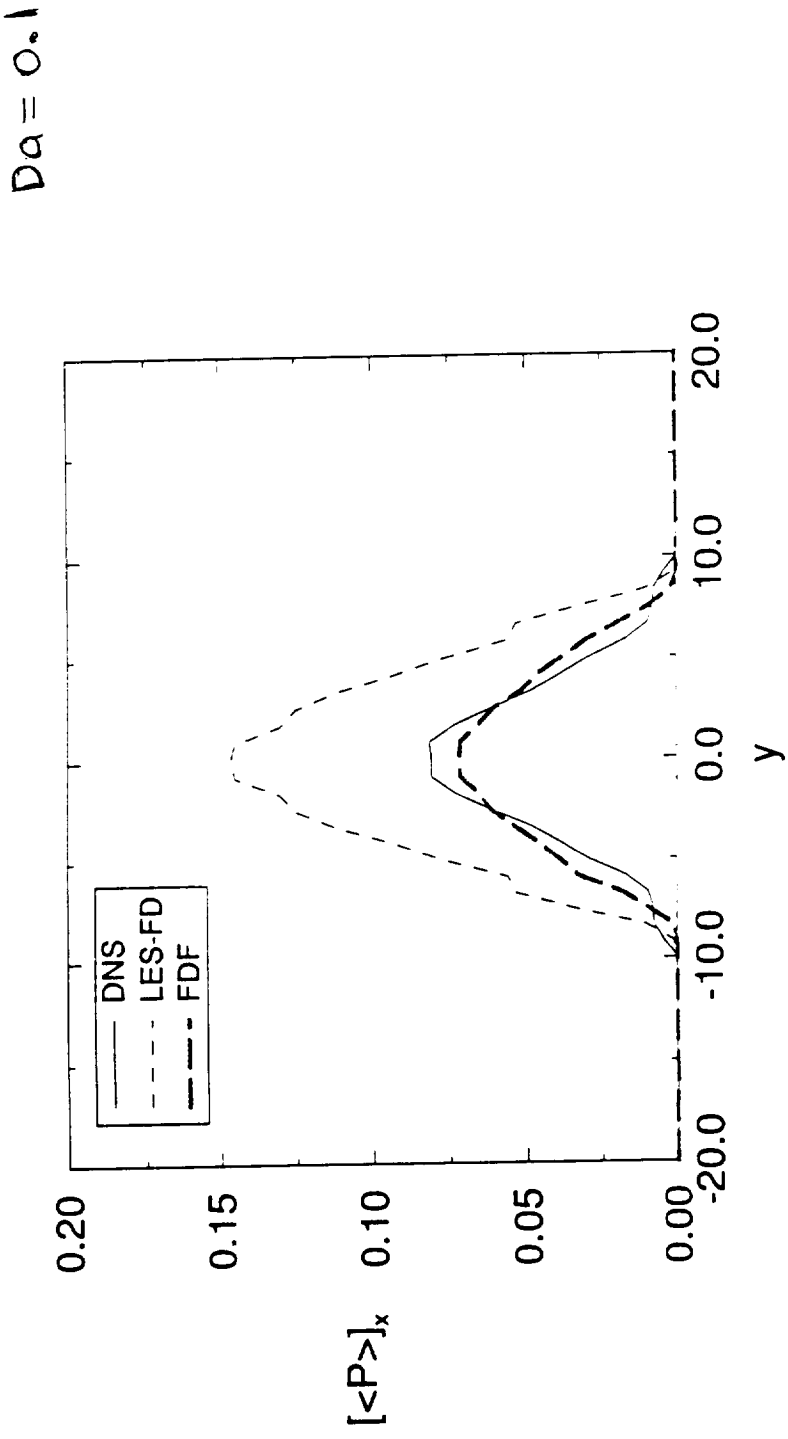

Figure 11 (a)

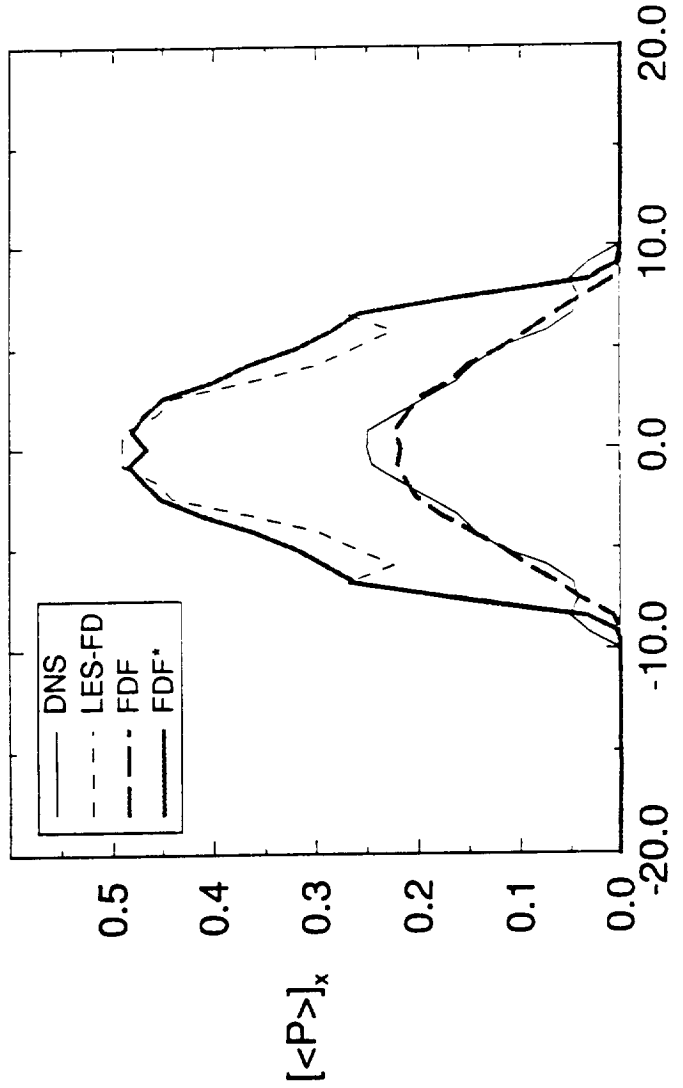

Figure 11 (b)

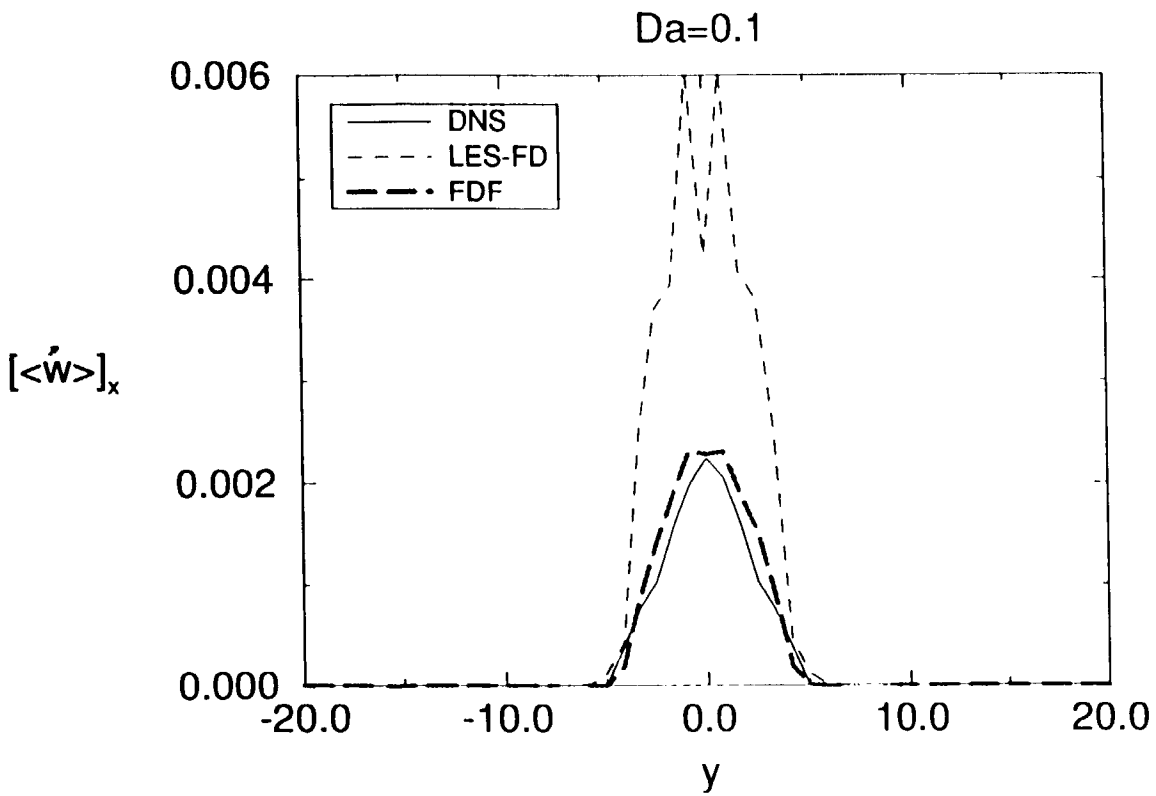

Figure 12 (a)

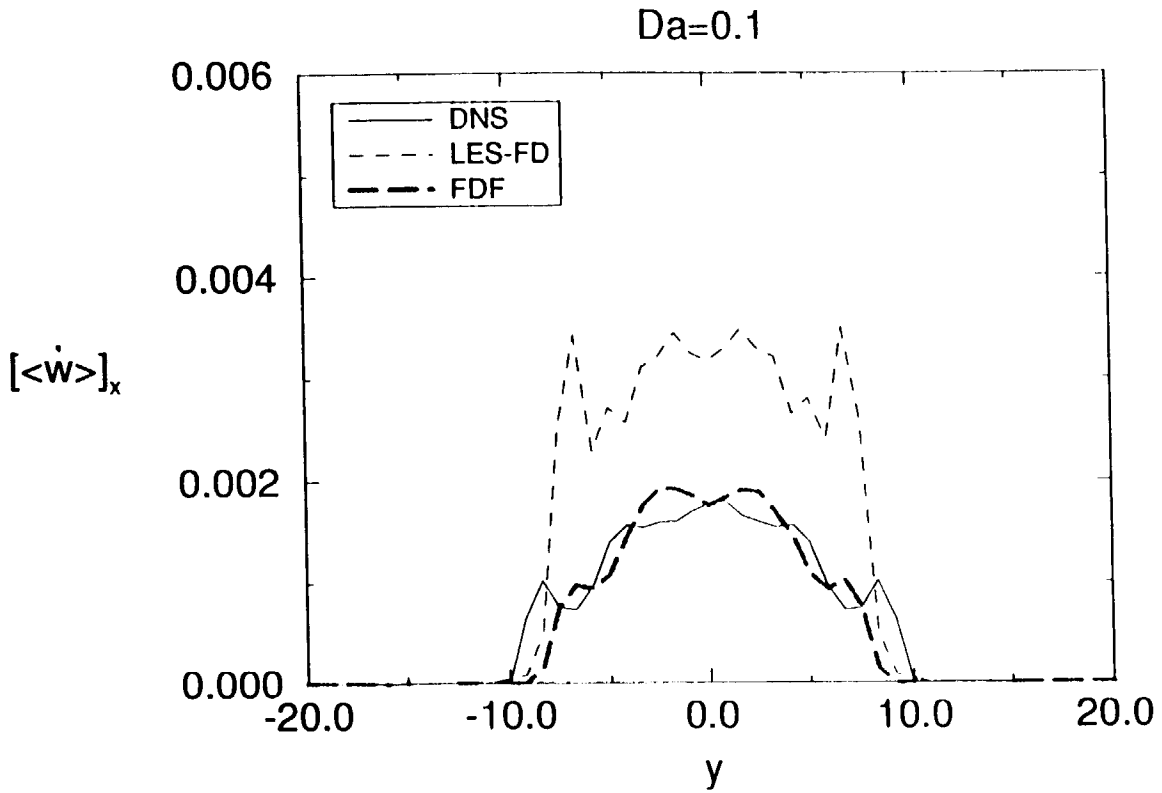
Da=0.1
DNS
LES-FD
FDF
0.006
0.004
0.002
0.000
$[\langle \dot{w} \rangle]_x$
-20.0
-10.0
0.0
10.0
20.0
y

Figure 12 (b)

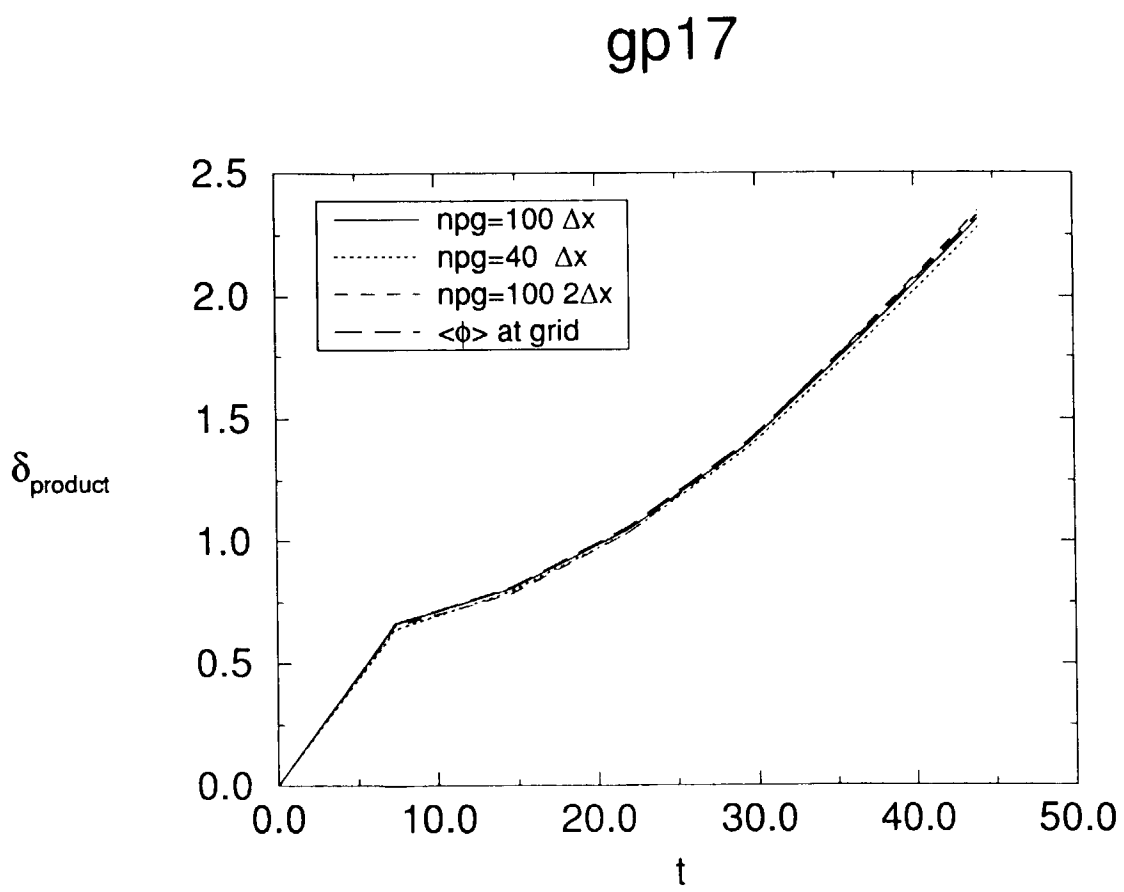
gp17
npg=100 Δx
npg=40 Δx
npg=100 2Δx
<φ> at grid
δproduct
t
0.0
0.5
1.0
1.5
2.0
2.5
0.0
10.0
20.0
30.0
40.0
50.0

Figure 13 (a)

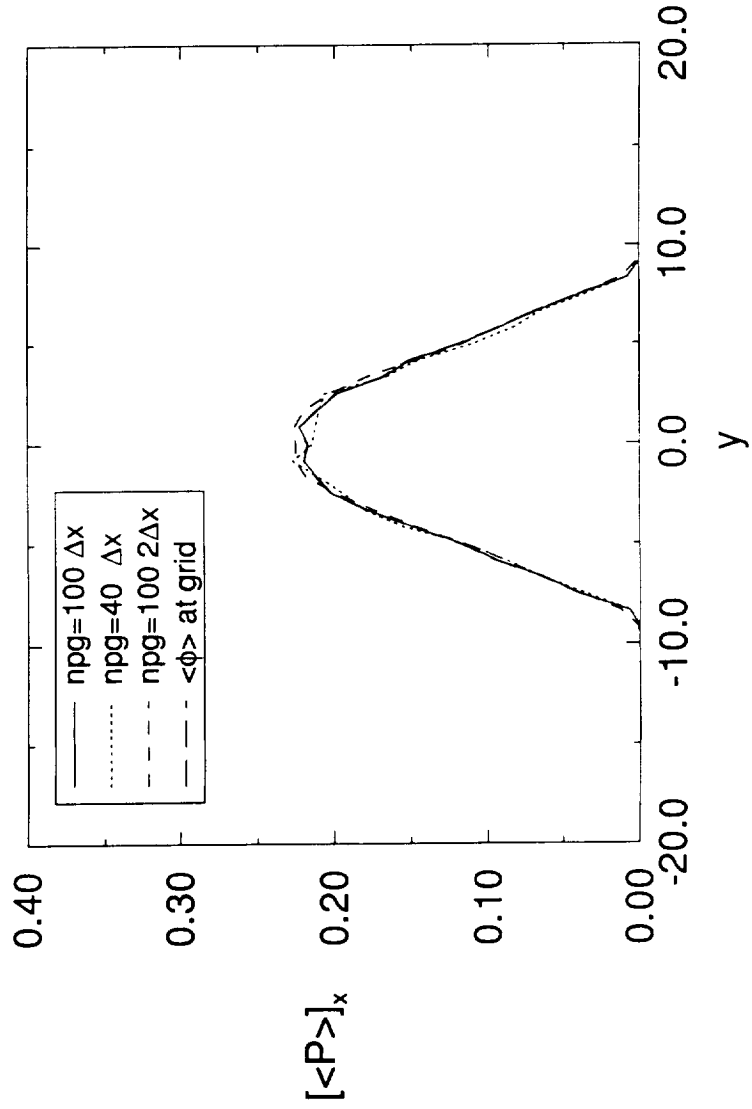
gp21
npg=100 Δx
npg=40 Δx
npg=100 2Δx
<φ> at grid
0.40
0.30
0.20
0.10
0.00
[<P>]x
-20.0
-10.0
0.0
10.0
20.0
y

Figure 13 (b)

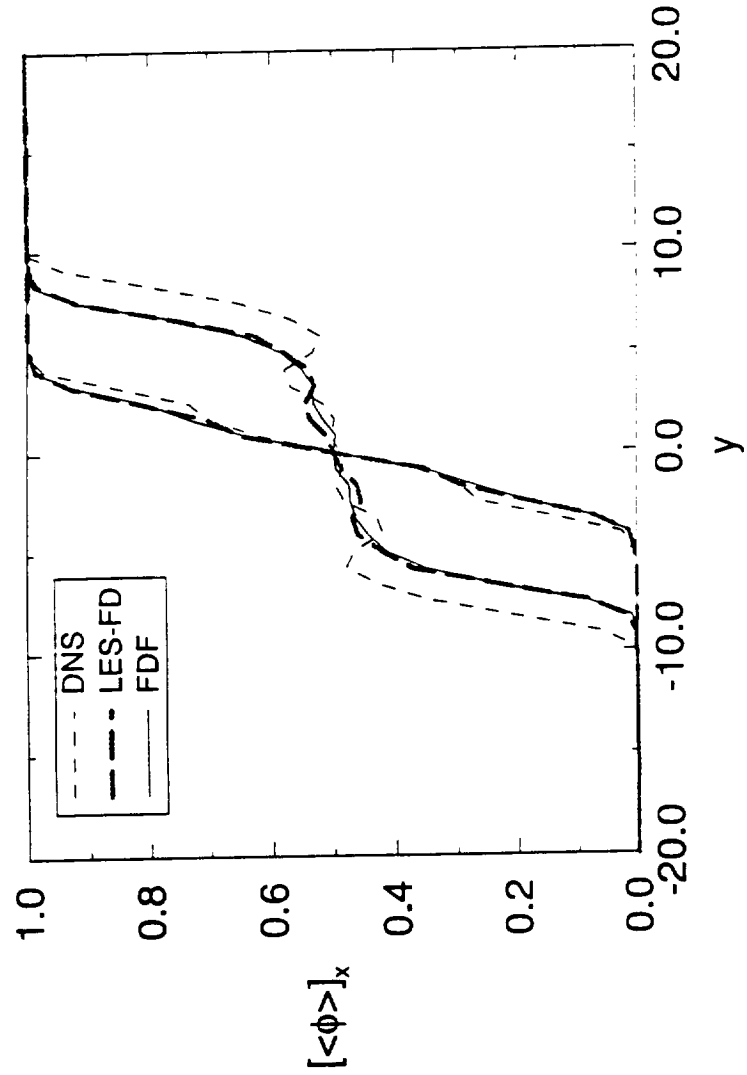
DNS
LES-FD
FDF
1.0
0.8
0.6
0.4
0.2
0.0
$[\langle\phi\rangle]_x$
-20.0
-10.0
0.0
10.0
20.0
y

Figure 14 (a)

Figure 14 (b)

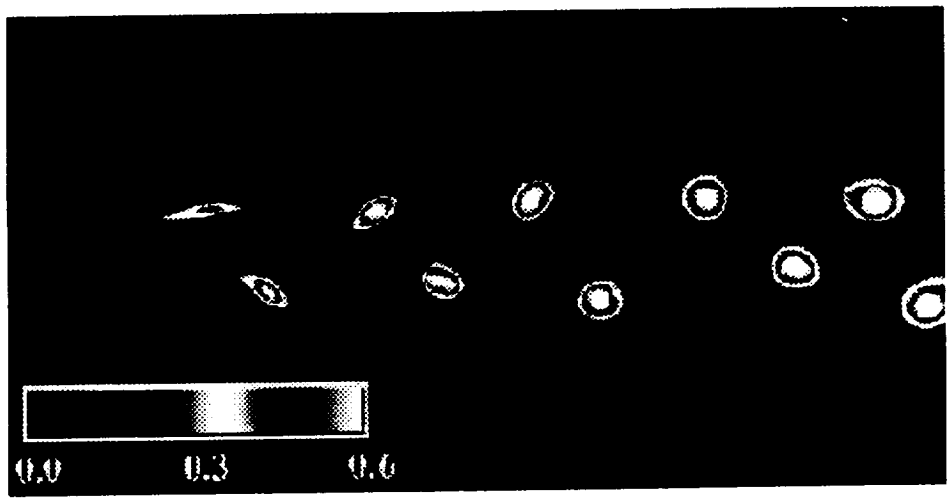

(a)

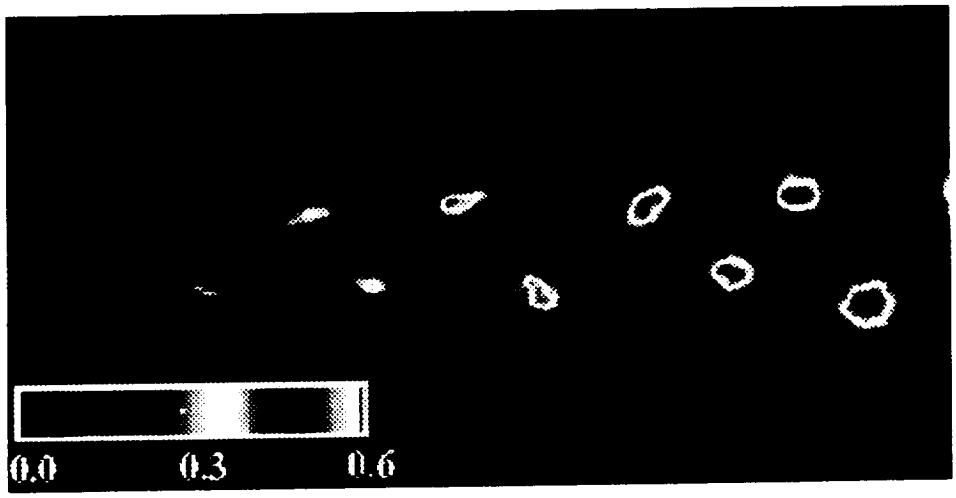

(b)

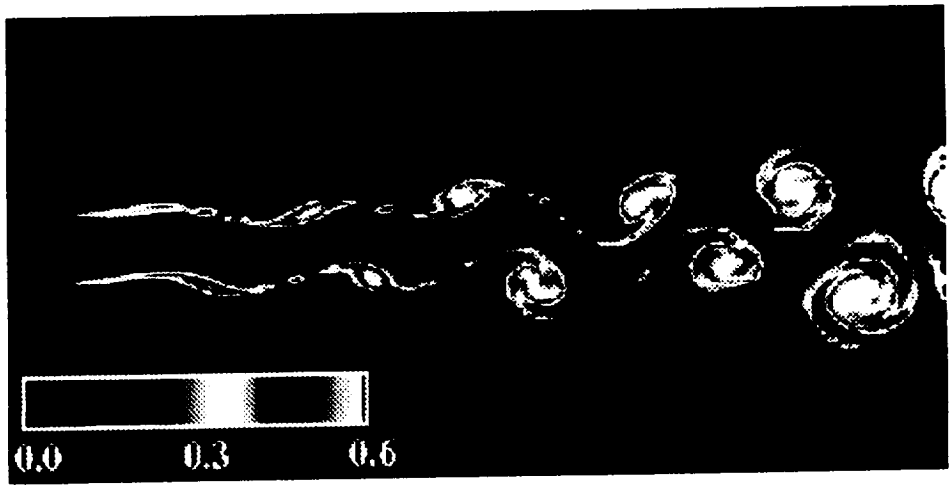

(c)

Fig. 15: Product mass fraction contours (a) DNS (b) FDF and (c) LES with no reaction model.

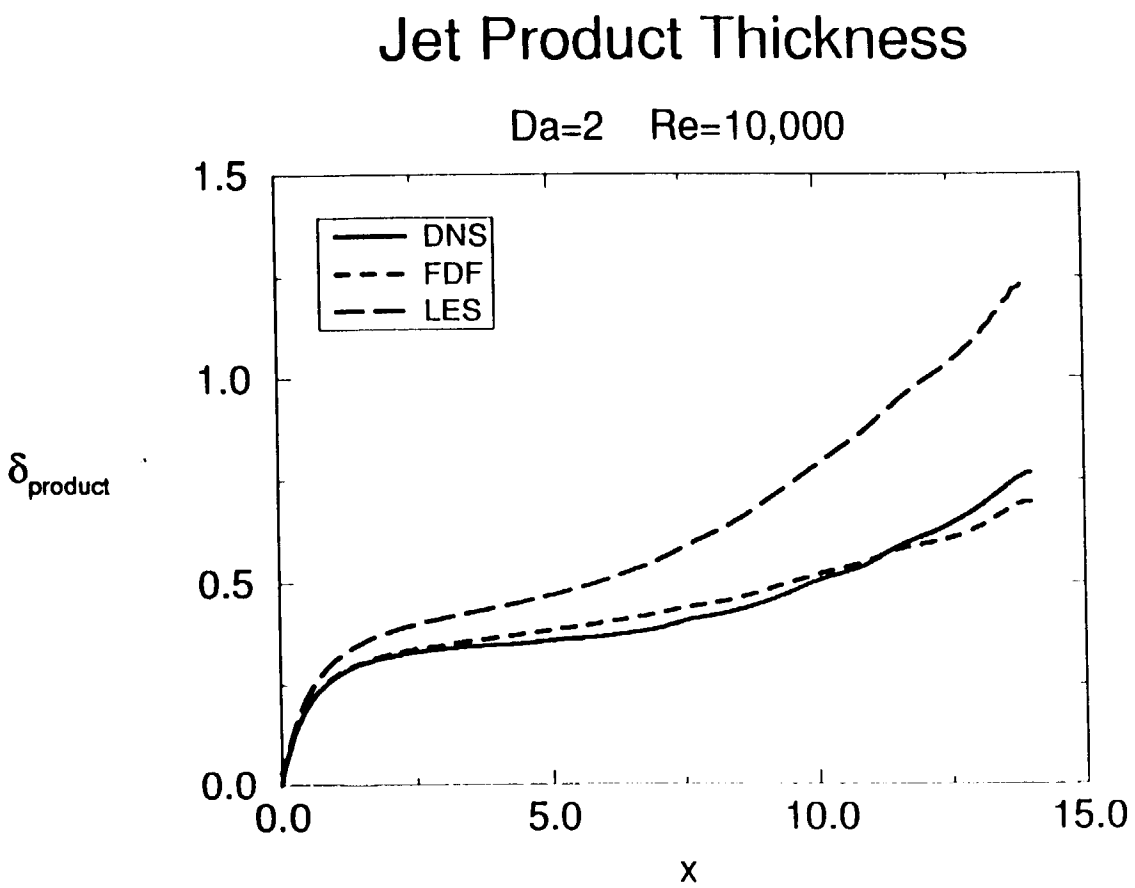
Jet Product Thickness
Da=2 Re=10,000
DNS
FDF
LES
$\delta_{product}$
1.5
1.0
0.5
0.0
0.0
5.0
10.0
15.0
x

Figure 16

Product Distribution
x=2D Re=10,000 Da=2.0
DNS
FDF
LES
0.80
0.70
0.60
0.50
0.40
0.30
0.20
0.10
0.00
[ϕp]t
-2.0
-1.0
0.0
1.0
2.0
y

Figure 17(a)

Product Distribution
x=7D Re=10,000 Da=2.0
DNS
FDF
LES
0.50
0.40
0.30
0.20
0.10
0.00
-2.0
-1.0
0.0
1.0
2.0
y
[φpl]

Figure 17 (b)

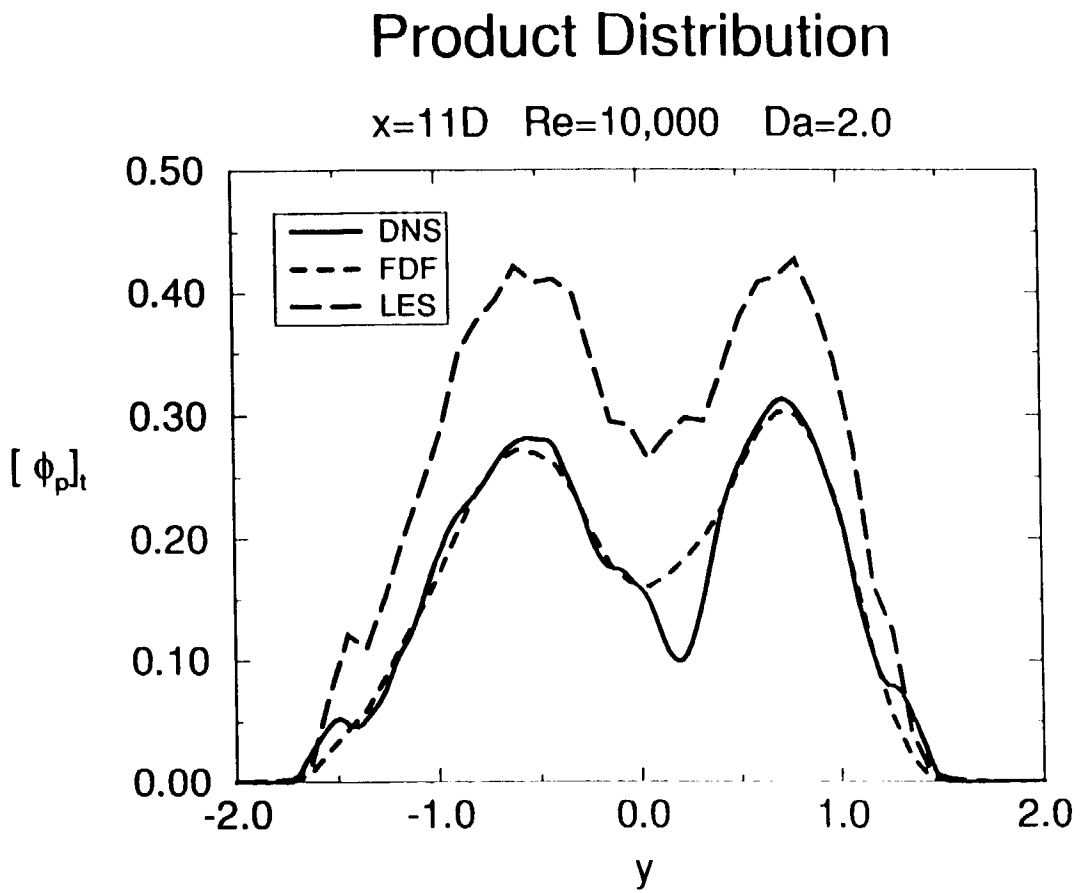
Product Distribution
x=11D Re=10,000 Da=2.0
DNS
FDF
LES
0.50
0.40
0.30
0.20
0.10
0.00
[φp]t
-2.0
-1.0
0.0
1.0
2.0
y

Figure 14 (c)